pMX-IG (22) using restriction endonucleases and a DNA ligation kit, version 1 (Takara BIO), to generate pMX-IG-PU.1.

Transfection

Infection of BMMC and PMC was performed, according to a previously reported method (12, 20). In brief, pMX-puro (mock vector) and pMX-puro-PU.1 (for the expression of wild-type PU.1) were transiently introduced into Plat-E with Fugene6 (Roche Diagnostics). BMMC after 4-wk culture and freshly prepared PMC were incubated with harvested culture medium of transfected Plat-E containing infectious viruses for 2 days in the presence of 10 μg/ml polybrene (Sigma-Aldrich). Infected cells were selected by culture in the presence of 1.2 μg/ml puromycin for 10–20 days. When pMX-IG and pMX-IG-PU.1 were used for transfection, transfectants that were obtained by the same method as that of pMX-puro-series described above were selected as GFP-positive cells.

Western blotting analysis

To detect endogenous PU.1, BMMC was stimulated by 1 μg/ml LPS or 100 mg/ml PMA (Sigma-Aldrich) for 0–48 h. Whole cells were subjected to Western blotting analysis. Rabbit polyclonal Ab against PU.1 (Santa Cruz Biotechnology) or mouse mAb against Flag-tag (Sigma-Aldrich) was used as the primary Ab. Alexa Fluor 680 goat anti-rabbit IgG or Alexa Fluor 680 goat anti-mouse IgG (Molecular Probes) was used as the secondary Ab. Infrared fluorescence on membranes was detected by Odyssey infrared imaging system (model ODY-9201-SC; LI-COR).

Flow cytometric analysis

The FITC- or PE-conjugated anti-mouse Abs against I-A^d, CD11b, CD11c, F4/80, and c-*kit*, all of which were purchased from BD Pharmingen, were used to stain each cell surface molecule after blocking Fc receptors with 2.4G2 (BD Pharmingen). Mouse IgE Ab (BD Pharmingen) conjugated with FITC was used to stain mouse FcεRI. To stain TLR2 and 4, anti-mouse TLR2 and 4 rat IgG mAbs purchased from HyCult Biotechnology were used as the first Ab, respectively, and FITC-conjugated rabbit $F(ab')_2$ anti-rat IgG Ab (Valeant Pharmaceuticals) was used as the second Ab. In the case of pMX-IG-series transfectants expressing GFP, cells were stained with PE-conjugated anti-mouse c-*kit* and allophycocyanin-conjugated anti-mouse CD11b, CD11c, or combination of biotin-labeled anti-mouse I-A^d and streptavidin-allophycocyanin (BD Pharmingen). For sorting of c-*kit*-positive or c-*kit*/FcεRI-double-positive cells, BD FACSAria Cell Sorter (BD Biosciences, San Jose, CA) was used. Cells stained with each Ab, as described previously (23, 24), were analyzed by FACSCalibur flow cytometer (BD Biosciences).

Morphological analysis

Electron microscopy and May-Grünwald-Giemsa's staining were performed, as described previously (12).

LPS, peptidoglycan (PGN), and Ag/IgE stimulation

Culture medium of cells stimulated with LPS (from *Escherichia coli*; Sigma-Aldrich), PGN (from *Staphylococcus aureus*; Sigma-Aldrich), or Ag/IgE was harvested after 6-h incubation. Stimulation with Ag/IgE was performed according to a previously published method (25). Concentrations of IL-6 in the culture supernatant were determined by an ELISA kit, according to the manufacturer's instruction (Genzyme Techne, Minneapolis, MN). β-Hexosaminidase-releasing assay was performed with previously reported method (25) to investigate degranulation activity.

Ag presentation assay

Cells irradiated at a dose of 30 Gy were plated into 96-well round-bottom plates at 5-fold serial dilutions, each well of which contained splenic $CD4^+$ T cells from C57BL/6 mice at 3×10^5, and incubated for 2 days. [^{3}H]Thymidine was then added (0.37 Mbq/well), and incubation was continued for an additional 15 h.

Results

Overproduction of PU.1 in BMMC induced the expression of MHC class II, CD11b, CD11c, and F4/80, and suppressed the expression of c-kit

To examine the effect of overproduced PU.1 in mast cells, BMMC were transfected with retrovirus vector that directed the production of wild-type PU.1 or empty vector (Fig. 1*A*). In Western blotting analysis using anti-PU.1 Ab (Fig. 1*B*), apparent production of wild-type PU.1 was observed, while endogenous PU.1 was not detected under the conditions used (see Fig. 1*B*, control (without transfection) and mock), indicating that the cells transfected with pMX-puro-PU.1 expressed much larger amount of PU.1 than that of endogenous PU.1. BMMC (*top panel* of Fig. 1*C*) and mock transfectants (*second panel* of Fig. 1*C*) expressed mast cell-specific markers (FcεRI and c-*kit*), but not monocyte-specific molecules (MHC class II, CD11b, CD11c, and F4/80; *bottom panel* of Fig. 1*C*) on cell surface. In contrast, overproduction of PU.1 in BMMC induced the expression of MHC class II, CD11b, CD11c, and F4/80, while the expression of c-*kit* was slightly suppressed (*third panel* of Fig. 1*C*). Significant difference was not observed in the expression level of FcεRI. These results indicated that overproduction of PU.1 in BMMC induced the expression of monocyte-specific molecules and suppressed c-*kit* expression.

Morphology of transfectants

To investigate the effect of PU.1 overproduction on the morphology of the cells, May-Grünwald-Giemsa staining of cytospun (Fig. 2*A*) and electron microscopy (Fig. 2*B*) were performed. The mock transfectants contained a large amount of granules as well as control BMMC. In contrast, PU.1-overproducing cells contained lesser amount of granules, but showed macrophage- and DC-like morphology characterized by vacuoles in the cytoplasm, larger veils, and lamellipodia extending from cell bodies. These observations showed that overproduction of PU.1 caused monocyte-like morphological change on BMMC.

Response to LPS and PGN stimulation

TLR4 signaling activated by LPS induces DC and macrophages to produce proinflammatory cytokines, including IL-6 (26). Although mast cells also produce IL-6 in response to LPS, the production level is quite lower than that of monocytes (27). We therefore analyzed the IL-6 production level of PU.1-overproducing cells by LPS stimulation (Fig. 3*A*). The amount of IL-6 produced by LPS stimulation was markedly increased in cells overproducing wild-type PU.1 as well as BMDC. In contrast, mock transfectants produced IL-6 at the level similar to that of BMMC.

To confirm the specificity of TLR signaling, we next analyzed the response to PGN, which activates cells via TLR2, by measuring IL-6 released from each transfectant (Fig. 3*B*). Overproduction of PU.1 resulted in markedly increased production of IL-6 in response to PGN stimulation.

Recently, it has been reported that the essential elements in the promoters of TLR2 and 4 genes were recognized by PU.1 (28, 29), suggesting the possibility that overproduction of PU.1 might enhance IL-6 production through increased expression of TLR2 and 4. We therefore analyzed cell surface expression of TLR2 and 4 in PU.1-overproducing cells (Fig. 3*C*). Although bone marrow-derived DC expressed an apparent amount of TLR2 and 4, PU.1-overproducing cells expressed TLR2 and 4 only slightly, which was similar to the case in BMMC.

These results suggest that PU.1 enhances IL-6 production by activating downstream process of TLR-LPS/PGN interaction in TLR signaling, but not by increasing the expression of TLRs.

Response to Ag/IgE stimulation

Mast cells also produce IL-6 in response to Ag/IgE stimulation through FcεRI. Although a certain kind of monocyte expresses FcεRI, the response of monocytes through FcεRI is markedly reduced in comparison with that of mast cells (30). To examine the effect of PU.1 on response to Ag/IgE stimulation, we analyzed the level of IL-6 production of the cells stimulated by Ag/IgE (Fig. 4*A*). The amount of IL-6 produced from PU.1-overproducing cells was markedly reduced when compared with the case of mock

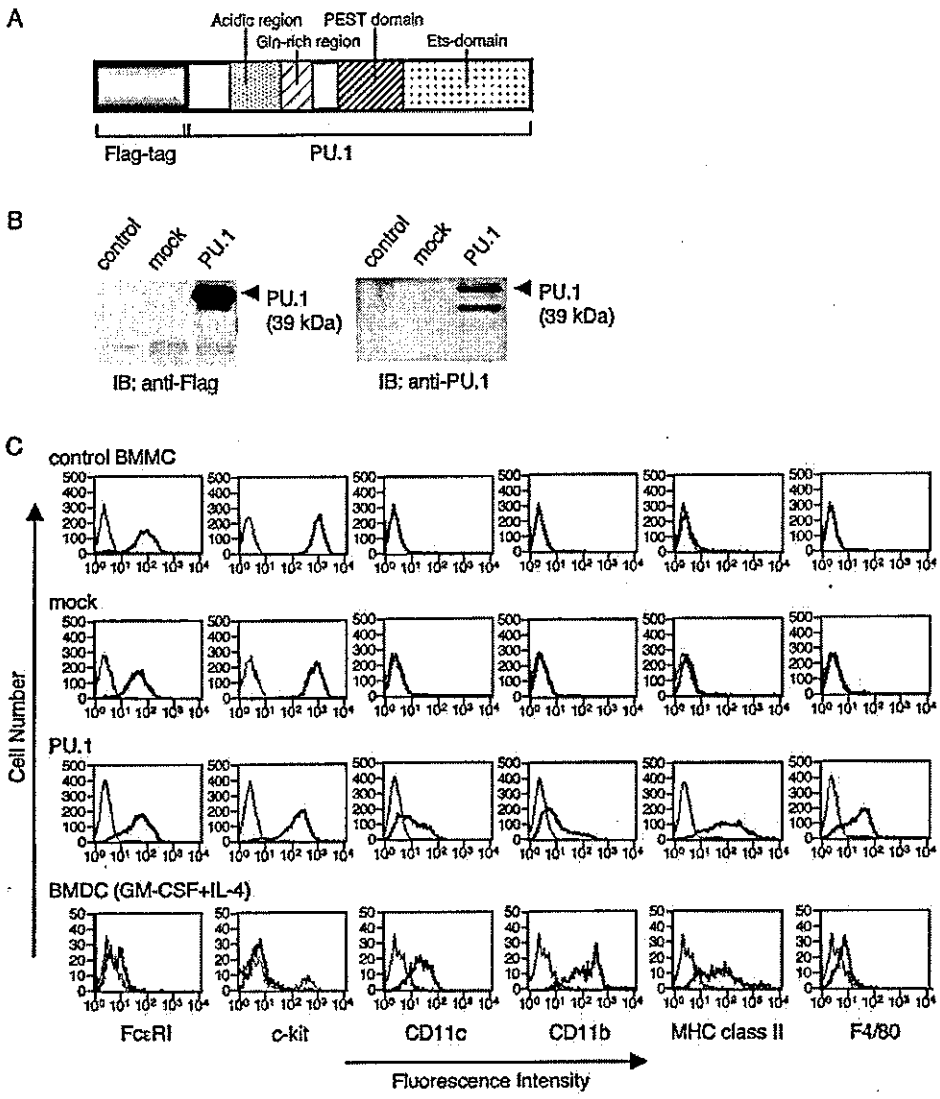

FIGURE 1. Overexpression of PU.1 in BMMC induces monocyte-specific gene expression. *A*, Schematic structure of PU.1. PU.1 is composed of the acidic region (33–73), the Gln-rich region (74–99), the Pro, Glu, Ser, and Thr-rich (PEST) region (117–166), and the Ets domain (167–271). The amino acid residue numbers are that of rat PU.1 numbering (21). PU.1 that is overproduced by retrovirus vector is tagged with 2× Flag at its N terminus. *B*, Western blotting analysis of BMMC and transfectants. A total of 5×10^5 cells was applied onto each lane. Control, normal BMMC after 6-wk culture; mock, BMMC transfected with mock vector (pMX-puro); PU.1, BMMC transfected with retrovirus vector encoding PU.1 cDNA (pMX-puro-PU.1). Transfectants were selected as puromycin-resistant cells by 10- to 20-day culture in the presence of puromycin (1.2 μg/ml). *C*, Cell surface expression of mast cell- and monocyte-specific molecules. Thick-line histogram represents cells with each Ab. Thin-line histogram indicates control with 2.4G2 alone. Control (*top panel*), normal BMMC without infection; mock (*second panel*), BMMC transfected with pMX-puro; PU.1 (*third panel*), BMMC transfected with pMX-puro-PU.1; BMDC (*bottom panel*), mouse BMDC. A representative result of five independent experiments is shown.

transfectants and control BMMC. This result indicated that overproduction of PU.1 reduced IL-6 production by interfering the signal from FcεRI.

Degranulation by cross-linking of FcεRI is one of the major characteristics of mast cells. Therefore, degranulation of the cells overproducing PU.1 was analyzed (Fig. 4*B*). Control BMMC and mock transfectants were degranulated by stimulation with Ag/IgE to the same degree. In contrast, degranulation of the cells overproducing PU.1 was markedly decreased as well as BMDC.

From these results, it was concluded that overproduction of PU.1 reduced response to the stimulation through FcεRI in mast cells.

T cell stimulation activity

Overproduction of PU.1 induced marked expression of MHC class II, which is a hallmark of APCs, on mast cells, as shown in Fig. 1*C*. To examine whether induced MHC class II possesses function, allostimulatory activity of transfectants cocultured with allogenic C57BL/6 $CD4^+$ T cells was measured. Thymidine incorporation of T cells was significantly increased when PU.1-overproducing cells were cocultured (Fig. 5).

Effect of overproduction of PU.1 on PMC

PMC is connective tissue-type mast cell, which is more maturated than mucosal-type mast cell, BMMC. To examine the effect of PU.1 on connective tissue-type mast cells, PU.1 was overexpressed in freshly isolated PMC by the retrovirus vectors. The expression level of PU.1 in transfectants was increased, as was the case in BMMC (data not shown). May-Grünwald-Giemsa staining indicated that overproduction of PU.1 caused morphological change of the cells: decrease in granules accompanied by formation of vacuoles, larger veils, and lamellipodia (Fig. 6*A*). Expression profile of the cell surface markers on PU.1-overproducing PMC (Fig. 6*B*) was somewhat different from the case of BMMC. Similar to the case in BMMC, CD11b and F4/80 were expressed and c-*kit* expression was suppressed on PU.1-overproducing PMC. However, expression of CD11c and MHC class II was not induced in the transfectant. Thus, increased expression of PU.1 induced several monocyte-like changes even in PMC, but the effect of PU.1 was negligible on some target molecules such as CD11b and MHC class II in PMC.

Transfection of sorted mast cells using internal ribosome entry site-GFP system to eliminate the contamination of monocyte lineages

Ten- to 20-day culture was required to select transfectants by puromycin, when plasmids pMX-puro-series were used for retrovirus transfection, as described above. Although the purity of mast cells is high (>95% for BMMC and >98% for PMC, as described in *Materials and Methods*), the possibility that monocytes and/or

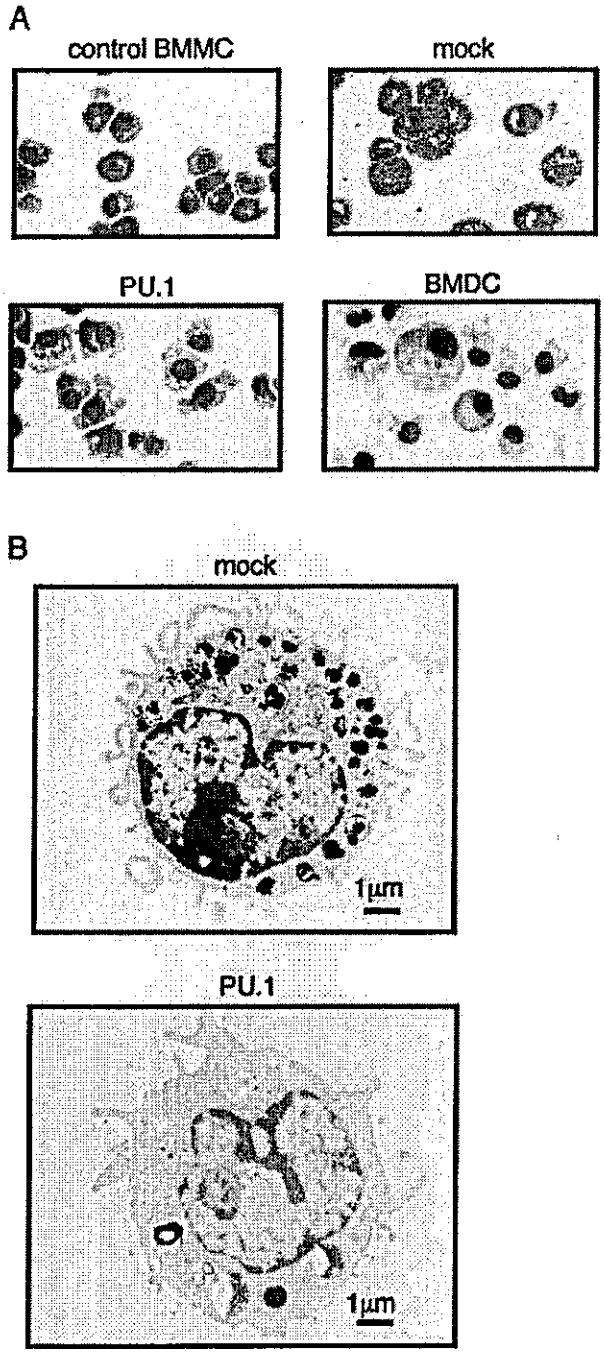

FIGURE 2. Morphology of control BMMC, each transfectant, and BMDC. *A*, May-Grünwald-Giemsa staining. ×1000. *B*, Electron micrographs; ×6000.

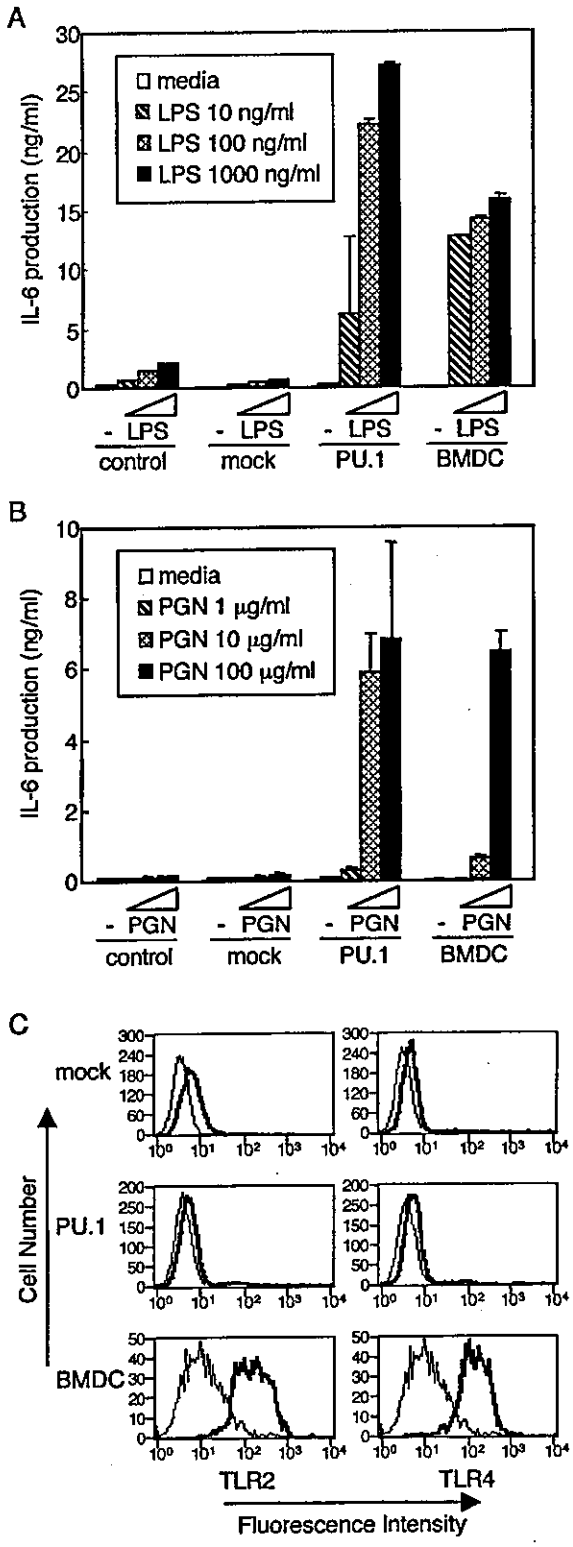

FIGURE 3. IL-6 production in response to the stimulation through TLR2 and 4. IL-6 production level in response to LPS stimulation (*A*) and PGN stimulation (*B*) was enhanced by overproduction of PU.1, whereas cell surface expression level of TLR2 and 4 was not affected by overproduction of PU.1 (*C*). *A* and *B*, IL-6 concentration in culture medium after 6 h of stimulation was measured by ELISA. A representative result performed with triplicate was shown as mean ± SD. Similar results were observed in other three independent experiments. *C*, Histogram of thick line represents cells stained with anti-TLR2 or 4 as first Ab and FITC-conjugated anti-rat IgG Ab as second Ab. Thin-line histogram indicates control cells incubated with second Ab alone. Similar profile was observed in another independent experiment.

monocyte progenitors contaminated mast cell suspensions could not be excluded completely. This issue raised a possibility that contaminating monocytes and/or monocyte progenitors that were transfected with retrovirus directing to produce PU.1 proliferated more vigorously than transfected mast cells in the culture period. Therefore, to eliminate this possibility, we used purified BMMC that was collected as c-*kit*$^+$/FcεRI$^+$ cells by sorting for transfection. After 14-day culture for selection of transfectants, >98% of mock transfectants were c-*kit*$^+$/FcεRI$^+$, while c-*kit*$^+$/FcεRI$^+$ population of ~94% was obtained from PU.1 transfectant (Fig. 7*A*). PU.1-overproducing cells expressed CD11c, CD11b, and MHC class II, which were not expressed on mock transfectants. These

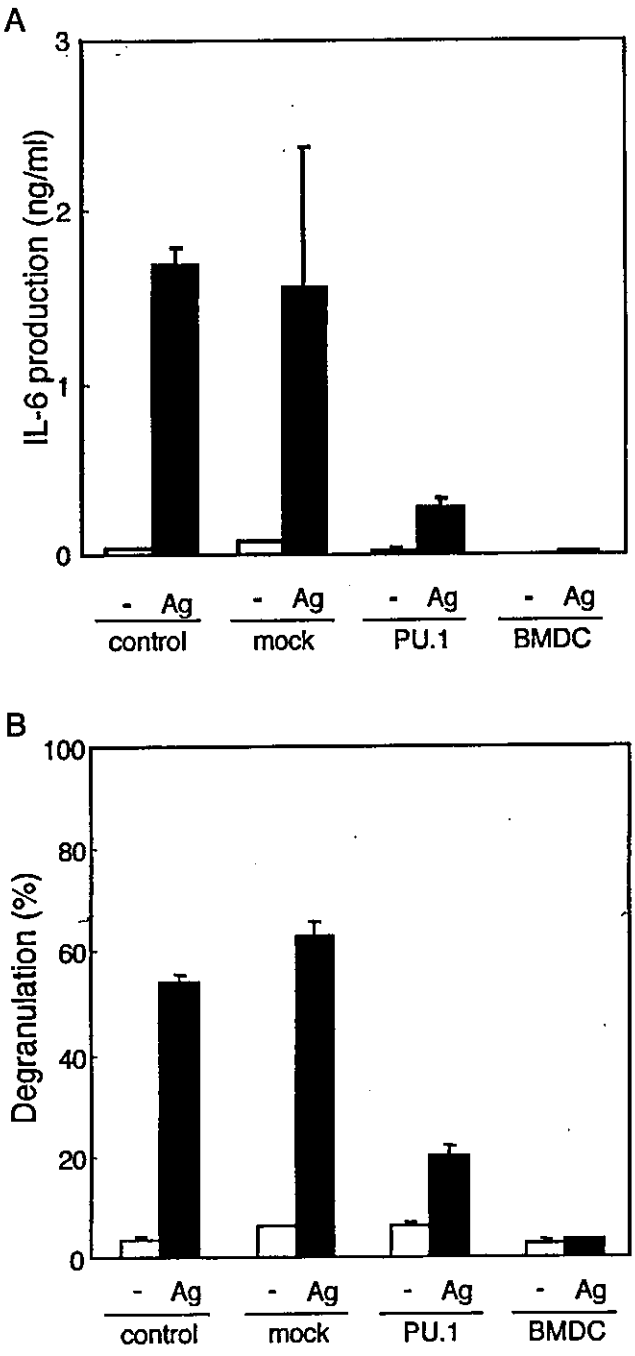

FIGURE 4. Response to Ag/IgE stimulation through FcεRI. *A*, IL-6 production of control or transfected BMMC. IL-6 concentration in culture medium after 6 h of stimulation by Ag/IgE was measured by ELISA. □, Cells were incubated with IgE Ab, but not following addition of Ag (DNP-BSA); ■, cells were cross-linked with Ag after incubation with IgE Ab. *B*, β-Hexosaminidase released from control or transfected BMMC. β-Hexosaminidase activity in supernatant was measured after 1-h incubation from stimulation by Ag/IgE. □, Cells were incubated with IgE Ab, but not following addition of Ag (DNP-BSA); ■, cells were cross-linked with Ag after incubation with IgE Ab. A representative result performed with triplicate was shown as mean ± SD in *A* and *B*. Similar results were observed in three other independent experiments.

results were consistent with the results of BMMC without sorting (Fig. 1*C*). In addition, CD11c-, CD11b-, and MHC class II-positive cells also expressed mast cell markers, c-*kit* and FcεRI. This result suggested that the cells expressing CD11c, CD11b, and MHC class II originated from mast cells.

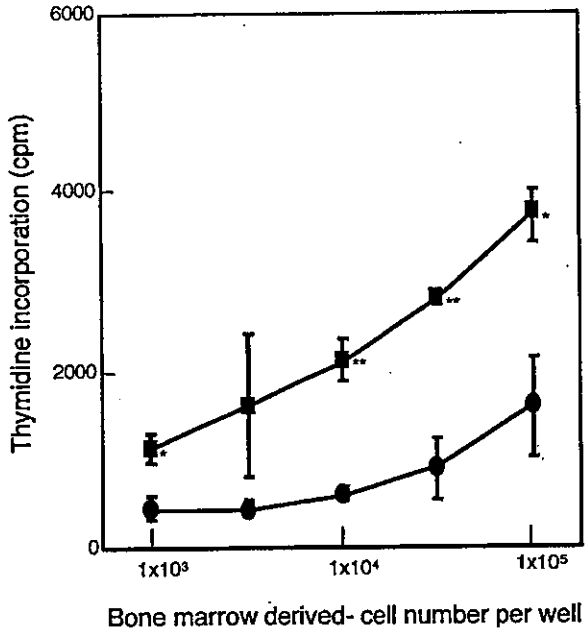

FIGURE 5. Effect of PU.1 on allostimulatory activity. Transfectants (H-2d) were irradiated and incubated with allogeneic $CD4^+$ T cells (H-2b) at the indicated concentrations. Proliferative responses of T cells were evaluated by the [^{3}H]thymidine incorporation of $CD4^+$ T cells. The results are expressed as mean ± SD of triplicate samples. *, $p < 0.005$; **, $p < 0.001$, as determined by a paired *t* test.

To eliminate the possibility that a few contaminating monocytes and/or its progenitors grew as a major population through 20 days of culture, we constructed plasmids, pMX-IG and pMX-IG-PU.1. By infection with retrovirus, transfectants were detected as GFP^+ cells within 2 days after transfection (Fig. 7*B*). GFP^+ population of BMMC infected with the retrovirus generated from pMX-IG-PU.1 showed reduced expression of c-*kit*, while GFP^- population and GFP^+ mock expressed c-*kit* at the level same as that of GFP^- mock. PU.1-overproducing cells detected as GFP^+ expressed CD11c and MHC class II, while most of the GFP^+ population of mock transfectants did not express these molecules. These observations excluded the possibility that contaminating monocytes were the source of cells expressing monocyte-specific molecules. From these results, we concluded that overproduction of PU.1 in BMMC suppressed c-*kit* expression and induced the expression of CD11c and MHC class II.

Up-regulation of endogenous PU.1 in mast cells by LPS or PMA stimulation

Because PU.1 autoregulates its own promoter (31), the stimulation signal to activate PU.1 protein would further accelerate overexpression of PU.1. Actually, the signal to activate PU.1 protein by LPS (32) and PMA (33) induces the up-regulation of PU.1 in monocytes. Therefore, we hypothesized that mast cells and/or its progenitors might be converted to monocyte-like cells in vivo under a certain condition when either activation or up-regulation of PU.1 is induced. To evaluate the effect of LPS and PMA on PU.1 expression level in mast cells, endogenous PU.1 proteins were analyzed after stimulation of mast cells with LPS or PMA by Western blotting. Intensity of the band migrating at ~39 kDa was markedly increased from 4 h after LPS or PMA stimulation and decreased to background level by 24-h incubation (Fig. 8). An additional band migrating slower than the major band of ~43 kDa also appeared from 4 to 8 h after LPS or PMA stimulation. Considering that PU.1 is shown to be present in several forms with

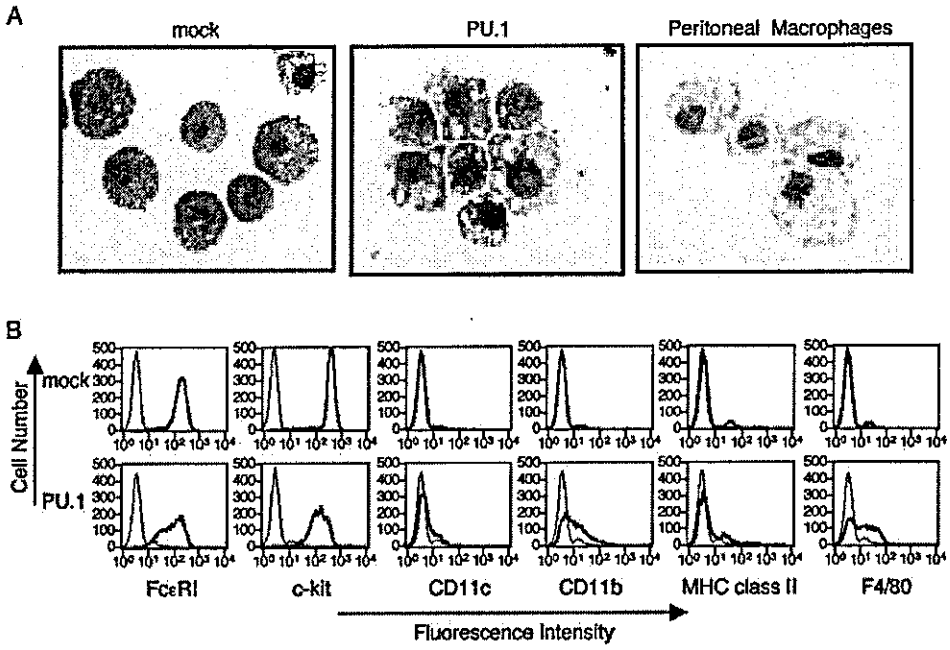

FIGURE 6. Overproduction of PU.1 in PMC. *A*, May-Grünwald-Giemsa staining of transfected PMC and peritoneal macrophages. ×1000. *B*, Cell surface expression of mast cell- or monocyte-specific molecules. Thick-line histogram represents cells with each Ab. Thin-line histogram indicates control with 2.4G2 alone.

various apparent molecular mass (from 38.5 to 46.5 kDa) (1), it is likely that proteins that were recognized by anti-PU.1 Ab are PU.1. Therefore, these results indicate that endogenous PU.1 in mast cells is potentially up-regulated in a certain condition, such as stimulation with LPS or PMA.

Discussion

PU.1 is a transcription factor involved in the lymphoid- and myeloid-specific gene regulation and the development of these cell lineages. Expression level of PU.1 determines cell fate between B cells/macrophages (8) and neutrophils/macrophages (9). In addition, overexpression of PU.1 in $CD34^+$ human myeloid progenitors promotes LC development (10, 11). In recent analysis, we found that monocyte-specific gene expression and monocyte-like morphological change were induced by overproduction of PU.1 in mouse bone marrow-derived mast cell progenitors (12, 20, 21). In this study, overproduction of PU.1 caused several monocyte-like characteristics on both BMMC and PMC, suggesting that developed mast cells still have the capacity to exhibit monocyte-like features.

Although the overproduction of PU.1 decreased the function and morphology of mast cells, PU.1 overproduction did not decrease the expression of FcεRI, a typical marker for mast cells. In most cases, PU.1 inhibits GATA-1 to function and vice versa, possibly by forming an inactive PU.1/GATA-1 complex (34), and therefore, only either PU.1 or GATA-1 is expressed in a cell. For example, in monocyte/granulocyte lineage development from hemapoietic stem cells, stimulation signals such as GM-CSF up-regulates PU.1 expression, which subsequently inhibits the function of GATA-1 in these cells (34–36). However, mast cells produce both PU.1 and GATA-1, and both transcription factors *trans* activate the promoter of FcεRI α-chain (37). GATA-1 also positively regulates the transcription of another FcεRI-specific component, FcεRI β-chain (38). In our present study, we observed that BMMC transfectants overproducing PU.1 still expressed GATA-1 at similar level as that of mock transfectants (data not shown). Therefore, we assume that GATA-1 present in the cell might assure FcεRI expression even in BMMC overproducing PU.1. The mechanism allowing the copresence of both GATA-1 and PU.1 in mast cells is unclear at present. Considering that cooperative function between GATA-1 and PU.1 is involved in mast cell-specific gene regulation (7, 37, 39), we speculate that this synergistic effect may be essential for mast cell development. In any case, further detailed analysis will be required to clarify these points.

Overproduction of PU.1 induced apparent expression of CD11b and F4/80, and suppressed c-*kit* expression in PMC. However, the PU.1 overproduction did not induce expression of CD11c and MHC class II in PMC, which was in contrast to the case of BMMC overproducing PU.1. These results indicated that PMC possessed lower capacity to express monocyte-specific gene than that of BMMC. We assume that this discrepancy may reflect the difference in the expression profile of other transcription factors between these cells. A transcription factor, C/EBPα, might be one of the candidates, because C/EBPα is reported to inhibit development of myeloid progenitor cells to DC, which is induced by PU.1, and direct them to macrophage and granulocyte lineages (11).

Overexpression of PU.1 in BMMC induced hyperproduction of IL-6 in response to stimulation signal through TLR2 and 4. It is suggested that PU.1 is involved in the transcriptional regulation of TLR2 and 4 (28, 29). However, expression level of TLR2 and 4 in BMMC was not affected by overproduction of PU.1 (Fig. 3). In addition, production of IL-6 in response to Ag/IgE stimulation was reduced (Fig. 4*A*). These results suggest that PU.1 regulates IL-6 expression in a complex manner. Considering that PU.1 is activated by stimulation with LPS (32), PU.1 might function in the downstream process in TLR signaling.

PU.1 autoregulates its own promoter (31). Therefore, the stimulation signal to activate PU.1 protein would further accelerate up-regulation of PU.1. Therefore, we hypothesize that mast cells and/or its progenitors might be converted to monocyte-like cells in vivo under a certain condition when either activation or overproduction of PU.1 is induced. We have shown that LPS and PMA stimulation induced PU.1 production in mast cells, which suggests that mast cells might be potential sources for macrophages and/or DC under certain conditions in vivo. This is the first observation in mast cells showing up-regulation of PU.1 by stimulation of LPS and PMA. However, the production of PU.1 induced by LPS or PMA stimulation was transient and markedly lower in level than that of PU.1 produced by retrovirus system. We assume that this is the reason for failure of the stimulations in converting mast cells to

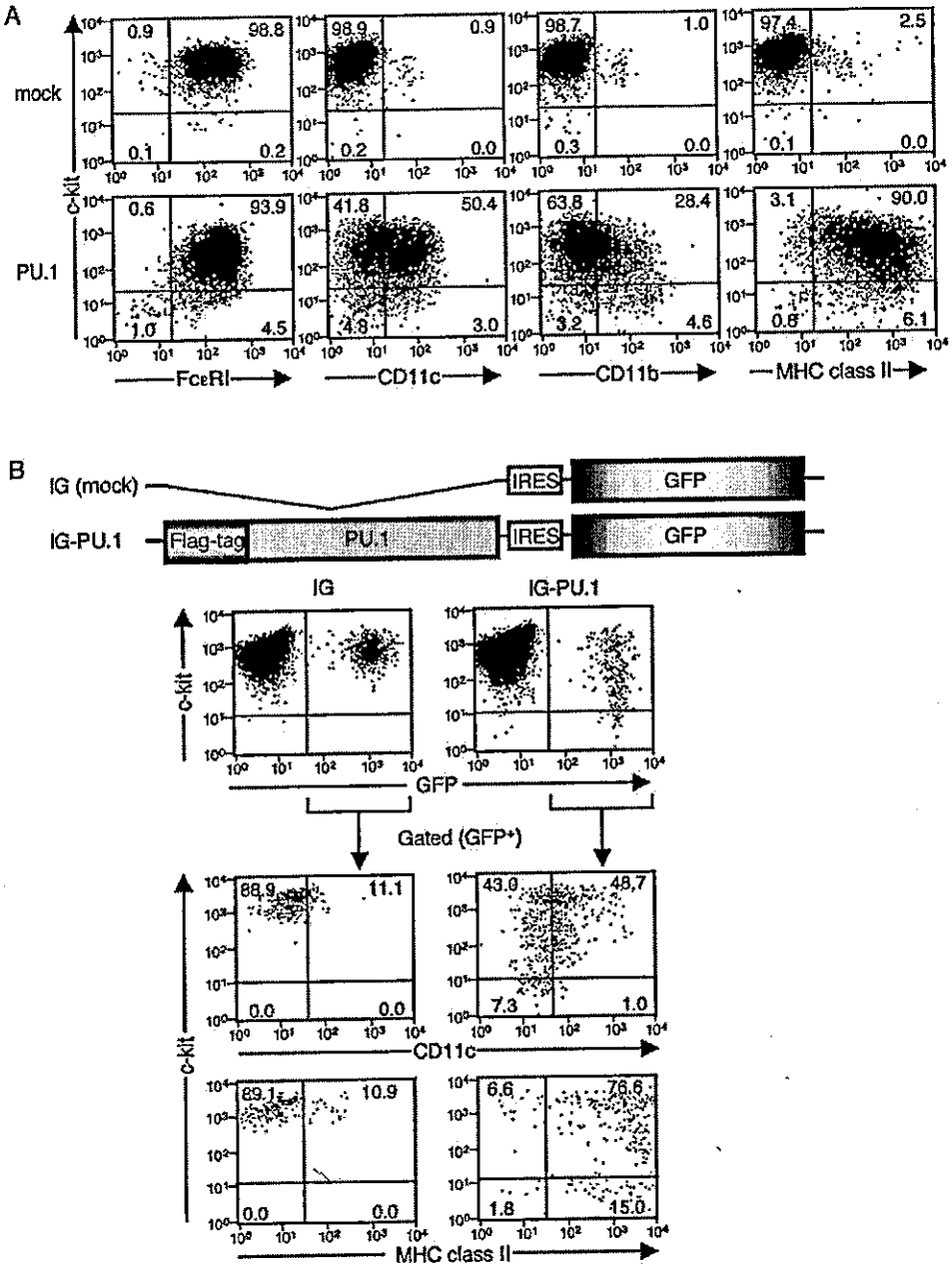

FIGURE 7. Effect of PU.1 overproduction on the expression of monocyte-specific markers for highly purified mast cells. *A*, Overproduction of PU.1 in BMMC highly purified by cell-sorting system with c-*kit*$^+$/FcεRI$^+$ as markers. c-*kit*$^+$/FcεRI$^+$ cells were transfected with pMX-puro or pMX-puro-PU.1. Transfectants resistant to puromycin were selected through 10-day culture in the presence of puromycin, and were double stained with PE-labeled anti-c-*kit* mAb and either FITC-labeled anti-FcεRIα, anti-CD11c, anti-CD11b, or anti-I-A^d mAb. *B*, PU.1-internal ribosome entry site (IRES)-GFP system. c-*kit*$^+$ cells collected by cell-sorting system were transfected with pMX-IG or pMX-IG-PU.1. Transfectants were monitored as GFP$^+$ cells 2 days after infection. Cells were double stained with PE-labeled anti-c-*kit* mAb and either allophycocyanin-labeled anti-CD11c mAb or biotinylated anti-I-A^d mAb, followed by allophycocyanin-labeled streptavidin. The GFP$^+$ populations in the *top panels* were electronically gated, and their dot plots of double stain were shown in the *middle panels* (PE-c-*kit* plus allophycocyanin-CD11c) and in the *bottom panels* (PE-c-*kit* plus biotin-I-A^d/allophycocyanin-avidin).

monocytes. To prove this possibility, further analysis will be required to optimize conditions of PU.1 induction in mast cells, which are suitable for obtaining monocyte-specific gene expression.

Recently, the presence in vivo of FcεRI-positive monocytes, DC, and LC, all of which possess the Ag presentation ability, was shown (40, 41). Considering that the marked up-regulation of FcεRI expression is observed specifically on LC and DC in lesional skin of atopic dermatitis (40, 41), we assume that above-mentioned signal to activate PU.1 might be a possible cause of the appearance of FcεRI-positive monocytes, which are developed from mast cells or its progenitors in vivo. Therefore, characterization of the mechanisms for the regulation of FcεRI expression on monocyte might give important information for prevention of atopic dermatitis.

GM-CSF (16) and M-CSF (42) induce development of hemopoietic progenitor cells toward DC and macrophage. In the process of monocyte development, the signal through these factors is transduced to Fes and subsequently to PU.1 (43) to induce the expression of the receptors for GM-CSF (44) and M-CSF (45). Actually, retrovirus-mediated expression of PU.1 in macrophage prepared from GM-CSF-null mice rescued the defect in differentiation (46). Thus, it is likely that PU.1-mediated gene expression is a key event in monocyte development. However, the mechanism for both activation of PU.1 and up-regulation of PU.1 expression is mostly unknown. Therefore, further detailed analyses on upstream and downstream signaling of PU.1 are required for revealing the mechanism for monocyte lineage development.

Acknowledgments

We thank Dr. M. Yoshida for electron microscopy, Dr. K. Yokomizo for May-Grünwald-Giemsa staining, Dr. T. Sakanishi for operating the cell-sorting system, and Drs. T. Kitamura and H. Nakano for providing Plat-E and pCR-2F, respectively. We are grateful to members of Atopy (Allergy) Research Center, Department of Immunology, and Department of Dermatology for helpful discussions, especially Drs. H. Yagita, A. Nakao (University of Yamanashi, Yamanashi, Japan), H. Ushio, H. Akiba, and T. Yamazaki. We thank Drs. N. Nakano, H. Kawada, A. Takagi, and A. Okamoto, and K.

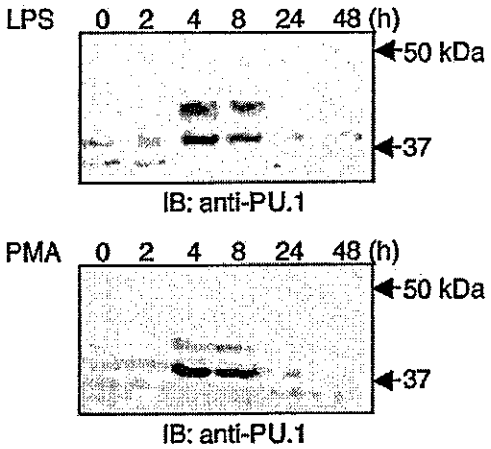

FIGURE 8. Up-regulation of endogenous PU.1 in mast cells by LPS or PMA stimulation. BMMC was incubated in culture medium in the presence of LPS (1 μg/ml) or PMA (100 mg/ml). Whole cells (1×10^6) were applied onto SDS-PAGE after 0- to 48-h incubation, as indicated at the *top* of each lane.

Fukuyama and T. Tokura for technical support, and M. Matsumoto and E. Kawasaki for secretarial assistance. We are grateful to Dr. W. Ng for proofing this manuscript.

References

1. Lloberas, J., C. Soler, and A. Celara. 1999. The key role of PU.1/SPI-1 in B cells, myeloid cells and macrophages. *Immunol. Today 20:184.*
2. McKercher, S. R., B. E. Torbett, K. L. Anderson, G. W. Henkel, D. J. Vestal, H. Baribault, M. Klemsz, A. J. Feeney, G. E. Wu, C. J. Paige, and R. A. Maki. 1996. Targeted disruption of the PU.1 gene results in multiple hematopoietic abnormalities. *EMBO J. 15:5647.*
3. Scott, E. W., M. C. Simon, J. Anastasi, and H. Singh. 1994. Requirement of transcription factor PU.1 in the development of multiple hematopoietic lineages. *Science 265:1573.*
4. Scott, E. W., R. C. Fisher, M. C. Olson, E. W. Kehrli, M. C. Simon, and H. Singh. 1997. PU.1 functions in a cell-autonomous manner to control the differentiation of multipotential lymphoid-myeloid progenitors. *Immunity 6:437.*
5. Anderson, K. L., H. Perkin, C. D. Surh, S. Venturini, R. A. Maki, and B. E. Torbett. 2000. Transcription factor PU.1 is necessary for development of thymic and myeloid progenitor-derived dendritic cells. *J. Immunol. 164:1855.*
6. Guerriero, A., P. B. Langmuir, L. M. Spain, and E. W. Scott. 2000. PU.1 is required for myeloid-derived but not lymphoid-derived dendritic cells. *Blood 95:879.*
7. Walsh, J. C., R. P. DeKoter, H.-J. Lee, E. D. Smith, D. W. Lancki, M. F. Gurish, D. S. Friend, R. L. Stevens, J. Anastasi, and H. Singh. 2002. Cooperative and antagonistic interplay between PU.1 and GATA-2 in the specification of myeloid cell fates. *Immunity 17:665.*
8. DeKoter, R. P., and H. Singh. 2000. Regulation of B lymphocyte and macrophage development by graded expression of PU.1. *Science 288:1439.*
9. Dahl, R., J. C. Walsh, D. Lancki, P. Laslo, S. R. Iyer, H. Singh, and M. C. Simon. 2003. Regulation of macrophages and neutrophil cell fates by the PU.1:C/EBPα ratio and granulocyte colony-stimulating factor. *Nat. Immunol. 4:1029.*
10. Iwama, A., M. Osawa, R. Hirasawa, N. Uchiyama, S. Kaneko, M. Onodera, K. Shibuya, A. Shibuya, C. Vinson, D. G. Tenen, and H. Nakauchi. 2002. Reciprocal roles for CCAAT/enhancer binding protein (C/EBP) and PU.1 transcription factors in Langerhans cell commitment. *J. Exp. Med. 195:547.*
11. Reddy, V. A., A. Iwama, G. Iotzova, M. Schulz, A. Elsasser, R. K. Vangala, D. G. Tenen, W. Hiddemann, and G. Behre. 2002. Granulocyte inducer C/EBPα inactivates the myeloid master regulator PU.1: possible role in lineage commitment decisions. *Blood 100:483.*
12. Nishiyama, C., M. Nishiyama, T. Ito, S. Masaki, K. Maeda, N. Masuoka, H. Yamane, T. Kitamura, H. Ogawa, and K. Okumura. 2004. Overproduction of PU.1 in mast cell progenitors: its effect on monocyte- and mast cell-specific gene expression. *Biochem. Biophys. Res. Commun. 313:516.*
13. Morita, S., T. Kojima, and T. Kitamura. 2000. Plat-E: an effieicnt and stable system for transient packaging of retroviruses. *Gene Ther. 7:1063.*
14. Nakahata, T., S. S. Spicer, J. R. Cantey, and M. Ogawa. 1982. Clonal assay of mouse mast cell colonies in methylcellulose culture. *Blood 60:352.*
15. Yurt, R. W., R. W. Leid, Jr., and K. F. Austen. 1977. Native heparin from rat peritoneal mast cells. *J. Biol. Chem. 252:518.*
16. Inaba, K., M. Inaba, N. Romani, H. Aya, M. Deguchi, S. Ikehara, S. Muramatsu, and R. M. Steinman. 1992. Generation of large numbers of dendritic cells from mouse bone marrow cultures supplemented with granulocyte/macrophage colony-stimulating factor. *J. Exp. Med. 176:1693.*
17. Labeur, M. S., B. Roters, B. Pers, A. Mehling, T. A. Luger, T. Schwarz, and S. Grabbe. 1999. Generation of tumor immunity by bone marrow-derived dendritic cells correlates with dendritic cell maturation stage. *J. Immunol. 162:168.*
18. Yamazaki, T., H. Akiba, H. Iwai, H. Matsuda, M. Aoki, Y. Tanno, T. Shin, H. Tsuchiya, D. M. Pardoll, K. Okumura, et al. 2002. Expression of programmed death 1 ligands by murine T cells and APC. *J. Immunol. 169:5538.*
19. Onishi, M., S. Konoshita, Y. Morikawa, A. Shibuya, J. Phillips, L. L. Lanier, D. M. Gorman, G. P. Nolan, A. Miyajima, and T. Kitamura. 1996. Applications of retrovirus-mediated expression cloning. *Exp. Hematol. 24:324.*
20. Nishiyama, C., M. Nishiyama, T. Ito, S. Masaki, N. Masuoka, H. Yamane, T. Kitamura, H. Ogawa, and K. Okumura. 2004. Functional analysis of PU.1 domains in monocyte-specific gene regulation. *FEBS Lett. 561:63.*
21. Nishiyama, C., N. Masuoka, M. Nishiyama, T. Ito, H. Yamane, K. Okumura, and H. Ogawa. 2004. Evidence against requirement of Ser41 and Ser45 for function of PU.1: molecular cloning of rat PU.1. *FEBS Lett. 572:57.*
22. Nosaka, T., T. Kawashima, K. Misawa, K. Ikuta, A. L.-F. Mui, and T. Kitamura. 1998. STAT5 as a molecular regulator of proliferation, differentiation and apoptosis in hematopoietic cells. *EMBO J. 18:4754.*
23. Hasegawa, M., C. Nishiyama, M. Nishiyama, Y. Akizawa, K. Takahashi, T. Ito, S. Furukawa, C. Ra, K. Okumura, and H. Ogawa. 2003. Regulation of the human FcεRI α-chain distal promoter. *J. Immunol. 170:3732.*
24. Nishiyama, C., Y. Akizawa, M. Nishiyama, T. Tokura, H. Kawada, K. Mitsuishi, M. Hasegawa, T. Ito, N. Nakano, A. Okamoto, et al. 2004. Polymorphisms in the *FcεRIβ* promoter region affecting transcription activity: a possible promoter-dependent mechanism for association between *FcεRIβ* and atopy. *J. Immunol. 173:6458.*
25. Furumoto, Y., S. Hiraoka, K. Kawamoto, S. Masaki, T. Kitamura, K. Okumura, and C. Ra. 2000. Polymorphisms in FcεRI β chain do not affect IgE-mediated mast cell activation. *Biochem. Biophys. Res. Commun. 273:765.*
26. Kaisho, T., and S. Akira. 2001. Dendritic-cell function in Toll-like receptor- and MyD88-knock out mice. *Trends Immunol. 22:78.*
27. Supajatura, V., H. Ushio, A. Nakao, K. Okumura, C. Ra, and H. Ogawa. 2001. Protective roles of mast cells against enterobacterial infection are mediated by Toll-like receptor 4. *J. Immunol. 167:2250.*
28. Rehli, M., A. Poltorak, L. Schwarzfischer, S. W. Krause, R. Andreesen, and B. Beutler. 2000. PU.1 and interferon consensus sequence-binding protein regulate the myeloid expression of the human Toll-like receptor 4 gene. *J. Biol. Chem. 275:9773.*
29. Haehnel, V., L. Schwarzfischer, M. J. Fenton, and M. Rehli. 2002. Transcriptional regulation of the human *Toll-like receptor 2* gene in monocytes and macrophages. *J. Immunol. 168:5629.*
30. Katoh, N., S. Kraft, J. H. Wessendorf, and T. Bieber. 2000. The high-affinity IgE receptor (FcεRI) blocks apoptosis in normal human monocytes. *J. Clin. Invest. 105:183.*
31. Chen, H. M., D. Ray-Gallet, P. Zhang, C. J. Hetherington, D. A. Gonzalez, D.-E. Zhang, F. Moreau-Gachelin, and D. G. Tenen. 1995. PU.1 (Spi-1) autoregulates its expression in myeloid cells. *Oncogene 11:1549.*
32. Lodie, T. A., J. Ricardo Savedra, D. T. Golenbock, C. P. V. Beveren, R. A. Maki, and M. J. Fenton. 1997. Stimulation of macrophages by lipopolysaccharide alters the phosphorylation state, conformation, and function of PU.1 via activation of casein kinase II. *J. Immunol. 158:1848.*
33. Carey, J. O., K. J. Posekany, J. E. deVente, G. R. Pettit, and D. K. Ways. 1996. Phorbol ester-stimulated phosphorylation of PU.1: association with leukemic cell growth inhibition. *Blood 87:4316.*
34. Rekhtman, N., F. Radparvar, T. Evans, and A. I. Skoultchi. 1999. Direct interaction of hematopoietic transcription factors PU.1 and GATA-1: functional antagonism in erythroid cells. *Genes Dev. 13:1398.*
35. Voso, M. T., T. C. Burn, G. Wulf, B. Lim, G. Leone, and D. G. Tenen. 1994. Inhibition of hematopoiesis by competitive binding of transcription factor PU.1. *Proc. Natl. Acad. Sci. USA 91:7932.*
36. Nerlov, C., and T. Graf. 1998. PU.1 induces myeloid lineage commitment in multipotent hematopoietic progenitors. *Genes Dev. 12:2403.*
37. Nishiyama, C., M. Hasegawa, M. Nishiyama, K. Takahashi, Y. Akizawa, T. Yokota, K. Okumura, H. Ogawa, and C. Ra. 2002. Regulation of human FcεRI α-chain gene expression by multiple transcription factors. *J. Immunol. 168:4546.*
38. Maeda, K., C. Nishiyama, T. Tokura, Y. Akizawa, M. Nishiyama, H. Ogawa, K. Okumura, and C. Ra. 2003. Regulation of cell type-specific mouse FcεRI β-chain gene expression by GATA-1 via four GATA motifs in the promoter. *J. Immunol. 170:334.*
39. Henkel, G., and M. A. Brown. 1994. PU.1 and GATA: components of a mast cell-specific interleukin 4 intronic enhancer. *Proc. Natl. Acad. Sci. USA 91:7737.*
40. Kraft, S., J. H. M. Weβendorf, D. Hanau, and T. Bieber. 1998. Regulation of the high affinity receptor for IgE on human epidermal Langerhans cells. *J. Immunol. 161:1000.*
41. Kraft, S., and T. Bieber. 2001. FcεRI-mediated activation of transcription factors in antigen-presenting cells. *Int. Arch. Allergy Immunol. 125:9.*
42. Clark, S. C., and R. Kamen. 1987. The human hematopoietic colony-stimulating factors. *Science 236:1229.*
43. Kim, J., and R. A. Feldman. 2002. Activated Fes protein tyrosine kinase induces terminal macrophage differentiation of myeloid progenitors (U937 cells) and activation of the transcription factor PU.1. *Mol. Cell. Biol. 22:1903.*
44. Hohaus, S., M. S. Petrovick, M. T. Voso, Z. Sun, Dong-Zhang, and D. G. Tenen. 1995. PU.1 (Spi-1) and C/EBPα regulate expression of the granulocyte-macrophage colony-stimulating factor receptor α gene. *Mol. Cell. Biol. 15:5830.*
45. Zhang, D. E., C. J. Hetherington, H. M. Chen, and D. G. Tenen. 1994. The macrophage transcription factor PU.1 directs tissue-specific expression of the macrophage colony-stimulating factor receptor. *Mol. Cell. Biol. 14:373.*
46. Shibata, Y., P.-Y. Berclaz, Z. C. Chroneos, M. Yoshida, J. A. Whitsett, and B. C. Trapnell. 2001. GM-CSF regulates alveolar macrophage differentiation and innate immunity in the lung through PU.1. *Immunity 15:557.*

Kidney International, Vol. 66 (2004), pp. 597–604

Smad3 deficiency attenuates renal fibrosis, inflammation, and apoptosis after unilateral ureteral obstruction

KUMI INAZAKI, YUTAKA KANAMARU, YUKO KOJIMA, NORIYOSHI SUEYOSHI, KO OKUMURA, KAZUNARI KANEKO, YUICHIRO YAMASHIRO, HIDEOKI OGAWA, and ATSUHITO NAKAO

Atopy (Allergy) Research Center, Juntendo University School of Medicine, Tokyo, Japan; Department of Pediatrics, Juntendo University School of Medicine, Tokyo, Japan; Division of Pathology, Central Laboratory of Medical Sciences, Juntendo University School of Medicine, Tokyo, Japan; and Department of Immunology, Faculty of Medicine, University of Yamanashi, Yamanashi, Japan

Smad3 deficiency attenuates renal fibrosis, inflammation, and apoptosis after unilateral ureteral obstruction.

Background. Transforming growth factor-β (TGF-β) has been implicated in the development of renal fibrosis induced by unilateral ureteral obstruction (UUO). However, there is little information on signaling pathways mediating TGF-β activity involved in molecular and cellular events leading to renal fibrosis induced by UUO. In this study, we sought to determine whether Smad3, a major signaling component of TGF-β, mediated renal fibrosis induced by UUO.

Methods. Renal fibrosis, inflammation, and apoptosis induced by UUO were macroscopically and histologically compared between wild-type mice and Smad3 null mice.

Results. Gross appearance of the kidney after UUO showed relatively intact kidney in Smad3 null mice [Smad3(−/−) mice] when compared with that of wild-type mice [Smad3(+/+) mice]. Renal interstitial fibrosis based on the interstitial area stained with Aniline-blue or Sirius red solution was significantly attenuated in the obstructed kidney of Smad3(−/−) mice when compared with that of Smad3(+/+) mice. Deposition of type I and type III collagens were also significantly reduced in the obstructed kidney of Smad3(−/−) mice. In addition, the numbers of myofibroblasts, macrophages, and CD4/CD8 T cells infiltrated into the kidney after UUO were significantly attenuated in the obstructed kidney of Smad3(−/−) mice when compared with that of Smad3(+/+) mice. Furthermore, terminal deoxynucleotidyltransferase-mediated deoxyuridine triphosphate (dUTP) nick-end labeling (TUNEL) staining after UUO showed significantly reduced number of tubular apoptotic cells in the obstructed kidney of Smad3(−/−) mice when compared with that of Smad3(+/+) mice. Endogenous Smad pathway was activated in the obstructed kidney after UUO in wild-type mice as judged by the increase of phosphorylated Smad2 or phosphorylated Smad2/3-positive cells in renal interstitial area.

Conclusion. Smad3 deficiency attenuated renal fibrosis, inflammation, and apoptosis after UUO, suggesting that Smad3 was a key molecule mediating TGF-β activity leading to real fibrosis after UUO.

Key words: Smad, UUO, fibrosis, inflammation, apoptosis.

Received for publication August 4, 2003
and in revised form January 28, 2004, and March 1, 2004
Accepted for publication March 19, 2004

Fibrosis of the tubulointerstitial compartment often accompanied by inflammation is a major factor in progressive loss of renal function in patients with a variety of kidney diseases [1, 2]. Unilateral ureteral obstruction (UUO) is a representative model of tubulointerstitial renal fibrosis that have many readily quantifiable cellular and molecular events during the initiation and progression of renal fibrosis such as inflammation and apoptosis [3]. Although many factors are involved in the pathophysiology of UUO [3], it is well accepted that transforming growth factor-β (TGF-β) is a key molecule for the development of tubulointerstitial fibrosis in UUO [3–10]. It is generally thought that TGF-β is involved in tissue fibrosis including renal fibrosis induced by UUO based on its capacity to induce extracellular matrix (ECM) production, differentiation from fibroblasts into myofibroblasts, and apoptosis [3, 8, 11–13]. However, there is little information on signaling pathways mediating TGF-β activity that leads to renal fibrosis induced by UUO.

Although TGF-β activates multiple intracellular signaling pathways, recent intense investigations have revealed that Smad proteins constitute the basic components of the core intracellular signaling cascade carrying TGF-β signals from the cell surface directly to the nucleus [14–16]. The activated TGF-β receptors phosphorylate Smad2 and Smad3, which form heterotrimeric complex with Smad4, respectively, and enter the nucleus, bind directly or indirectly to DNA, and regulate transcription of many TGF-β target genes in cooperation with various transcriptional factors and coactivators/corepressors. Respective role of Smad2 and Smad3 in TGF-β signaling remains obscure, but reports on Smad2- and Smad3-deficient mice suggest a distinct role of Smad2 and Smad3 in vivo. Smad3 null mutant mice have been generated in

different laboratories [17–19], which were viable and fertile, in contrast to Smad2 null mice that show early embryonic lethality [20–22]. So far, the in vivo role of Smads in renal fibrosis has not been addressed.

In this study, we determined whether Smad3 played a role in the development of renal fibrosis in UUO by using Smad3-deficinet mice. We found that Smad3 deficiency attenuated renal fibrosis, inflammation, and apoptosis after UUO. Our findings suggest that Smad3 is a key molecule for cellular and molecular events involved in UUO and may thus become a novel therapeutic target for renal fibrosis.

METHODS

Mice

The generation of Smad3^{delEx8} null mice [Smad3(−/−) mice] by homologous recombination was described previously [17] and kindly provided by C. Deng (National Institutes of Health, Bethesda, MD, USA). In this line of mice, exon 8 of the Smad3 gene is deleted. The deletion removes the L3 loop, which is necessary for interaction with the TGF-β receptors, and the COOH-terminal serine-serine-valine-serine (SSVS) consensus phosphorylation site. Smad3(−/−) mice were backcrossed for six generations to C57BL6 mice as previously described [23]. Mice heterozygous for the targeted disruption were intercrossed to produce homozygous offspring and kept under specific pathogen-free conditions in the animal facility of Juntendo University.

Experimental design

Left kidney UUO was performed in male wild-type Smad3(+/+) mice and Smad3(−/−) mice, 10 to 12 weeks of age (N = 6 per group), as previously described [24]. Briefly, under anesthesia with pentobarbital sodium (0.3mg/g), UUO was created by complete double ligation of the left ureter with 2-0 silk suture through an abdominal midline incision. The mice were killed 14 days after UUO and the obstructed or intact right kidney was immediately weighed, and were fixed in 20% formalin and embedded in paraffin. Some portions of the kidney were immediately frozen in Tissue-Tek 22-oxacalcitriol (OCT) compound for immunohistochemical analysis. All animal experiments were performed according to the approved manual of the Institutional Review Board of Juntendo University. Preliminary studies confirmed that there were little renal fibrosis, inflammation, and apoptosis in sham-operated left kidney of Smad3(+/+) and Smad3(−/−) mice 14 days after the operation.

Histologic examination

The kidney sections (4 μm-thick) were stained with hematoxylin and eosin, periodic acid-Schiff, Aniline-blue, or Sirius red solutions. The severity of interstitial renal fibrosis was evaluated by the calculation of the positive area of Aniline-blue or Sirius red staining of one slide section measured with a computerized image analyzer (KS400) (Carl Zeiss Vision GmbH, Hallbergmoos, Germany).

Immunohistochemical staining

Interstitial cellularity or collagen deposition was characterized and quantified after immunoperoxidase staining for macrophages with F4/80 rat antimouse macrophage monoclonal antibody (Serotec Ltd., Oxford, UK), for myofibroblasts with peroxidase-conjugated murine antihuman α-smooth muscle actin (α-SMA) 1A4 monoclonal antibody (Dako Corp., Carpinteria, CA, USA), for T cells with rat antimouse CD4 and CD8 antibodies (BD Pharmingen, San Diego, CA, USA), and for collagens with antibodies against type I or type III collagen (Southern Biotechnology, Birmingham, AL, USA). Phosphorylated Smad2 or Smad2/3 expression in renal tissue was immunohistochemically detected by using antibodies against phosphorylated Smad2 (Cell Signaling Technology Inc., Beverly, MA, USA) or antiphosphorylated Smad2/3 (Santa Cruz Biotechnology, Santa Cruz, CA, USA). Sections with secondary antibody alone were negative. Scoring of F4/80-postive cells was determined to be 0, <5% of positive area in one high power field (×400); 1, 5% to 25% of positive area; 2, 25% to 50% of positive area; and 3, 50% to 75% of positive area; and 4, >75% of positive area. Random six high power fields were selected and scored. The number of CD4 or CD8-positive interstitial cells was counted manually in six random high power fields. α-SMA–positive area was measured with a computerized image analyzer (KS400) (Carl Zeiss Vision GmbH) as described above.

TUNEL assay

In situ detection of DNA fragmentation was performed using terminal deoxynucleotidyltransferase-mediated deoxyuridine triphosphate (dUTP) nick-end labeling (TUNEL) staining using in situ tunnel staining kit (Takara Bio, Inc., Ohtsu, Shiga, Japan) according to the manufacturer's recommendation. The number of TUNEL-positive cells was counted in six random high power fields.

Data analysis

Statistical analysis was performed using an unpaired the Student t test. Data were shown as mean ± SD and $P < 0.05$ was considered to be significant.

RESULTS

Phenotype of Smad3 null mice

A significant fraction (~50%) of Smad3(−/−) mice kept in our specific pathogen-free facility developed a

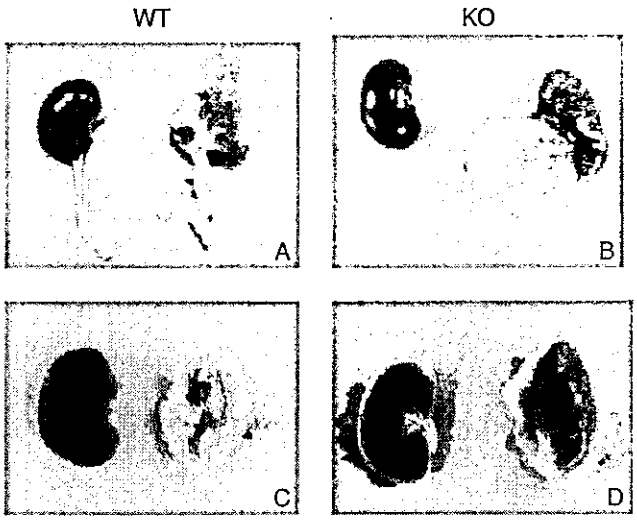

Fig. 1. Gross appearance of the mouse kidney 14 days after unilateral ureteral obstruction (UUO). The left obstructed kidney or right nonobstructed kidney of Smad3(+/+) and Smad3(−/−) mice were removed 14 days after UUO. Representative pictures of the kidneys from Smad3(+/+) mice (*A* and *C*) and from Smad3(−/−) mice (*B* and *D*) were shown. (C and D) Cross-section of the left and right kidneys. Note that the obstructed kidney of Smad3(−/−) mice showed relatively intact kidney tissue (much less whitish scar area than that of Smad3(+/+) mice). Abbreviations are: WT, wild-type; KO, knockout.

wasting syndrome associated with impaired mucosal immunity and abscess formation, and died between 1 and 4 months of age as previously described [17]. Yang et al [17] described that Smad3(−/−) mice exhibited reduced size compared with their littermate controls and developed bacterial abscesses near eyes, mandible, salivary glands, and intestine. This phenotype could be attributed, at least in part, to impaired chemotactic response of neutrophils toward TGF-β because the presence of neutrophils within the abscesses was few [17]. These mice were not used for the analysis. However, the remaining Smad3(−/−) mice appeared to develop normally, although slightly smaller than their littermates, and lived for at least 4 to 8 months. The kidneys of these mice were histologically intact and serum blood urea nitrogen (BUN) and creatinine levels were normal at the age of 10 to 12 weeks (data not shown). Thus, we decided to use these mice for the following studies and matched the Smad3(−/−) mice for weight as closely as possible with their wild-type controls.

Renal fibrosis

To determine whether Smad3 deficiency affected renal fibrosis in vivo, the severity of renal fibrosis and inflammation caused by UUO was compared in Smad3 wild-type (+/+) and Smad3-deficient (−/−) mice. Smad3(+/+) and Smad3(−/−) mice that underwent UUO were sacrificed for evaluation of renal lesion 14 days after UUO. As shown in Figure 1, gross appearance showed remarkable

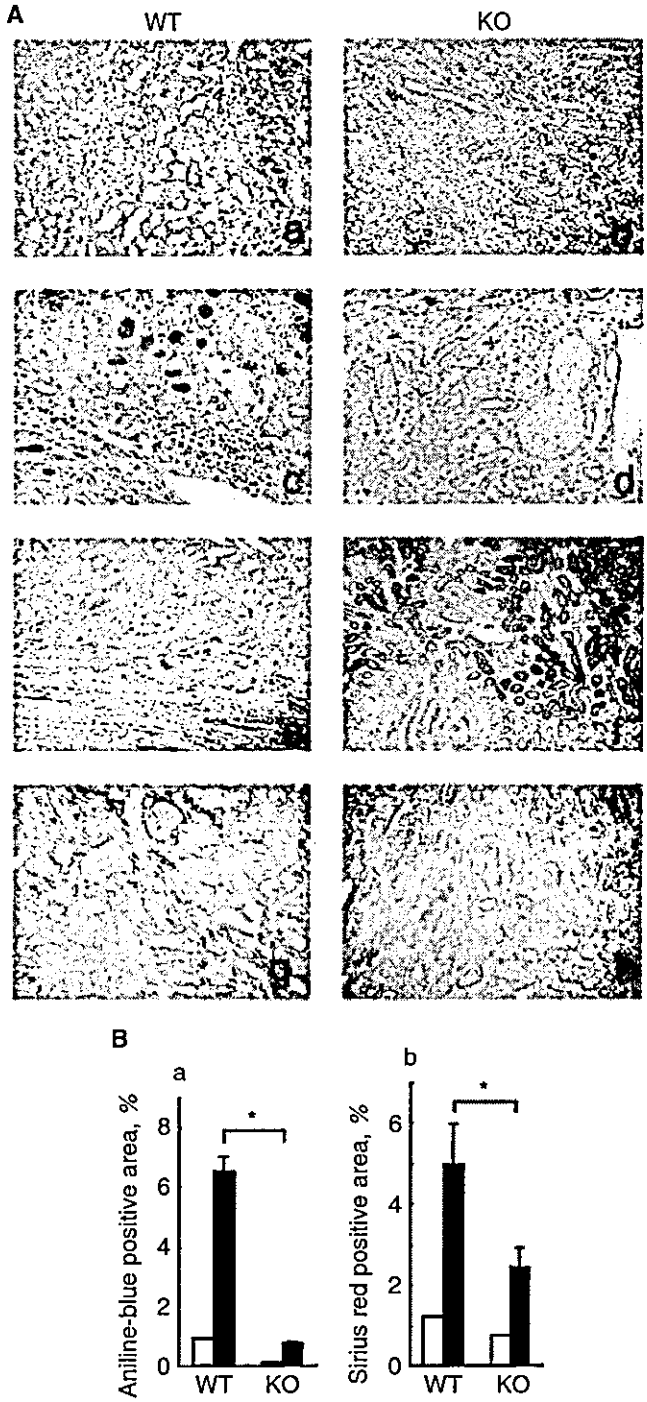

Fig. 2. Renal histology of the obstructed kidney after unilateral ureteral obstruction (UUO). (*A*) The left obstructed kidney were removed from Smad3(+/+) and Smad3(−/−) mice 14 days after UUO and the kidney sections were prepared and stained with hematoxylin-eosin (a and b), periodic acid-Schiff (c and d), Aniline-blue (e and f), or Sirius red (g and h) solutions. Representative pictures of the kidneys from Smad3(+/+) mice (a, c, e, and g) and from Smad3(−/−) mice (b, d, f, and h) are shown. (*B*) Quantitative analysis of Aniline-blue or Sirius red staining. The Aniline-blue (a) or Sirius-red (b) positive area of one slide of the left obstructed (■) or nonobstructed right kidney (□) of Smad3(+/+) mice [wild-type (WT)] and Smad3(−/−) mice [knockout (KO)] 14 days after UUO was measured with a computerized image analyzer as described in the **Methods** section. Results were expressed as percentage of positive area of one slide ($N = 6$). $^*P < 0.05$.

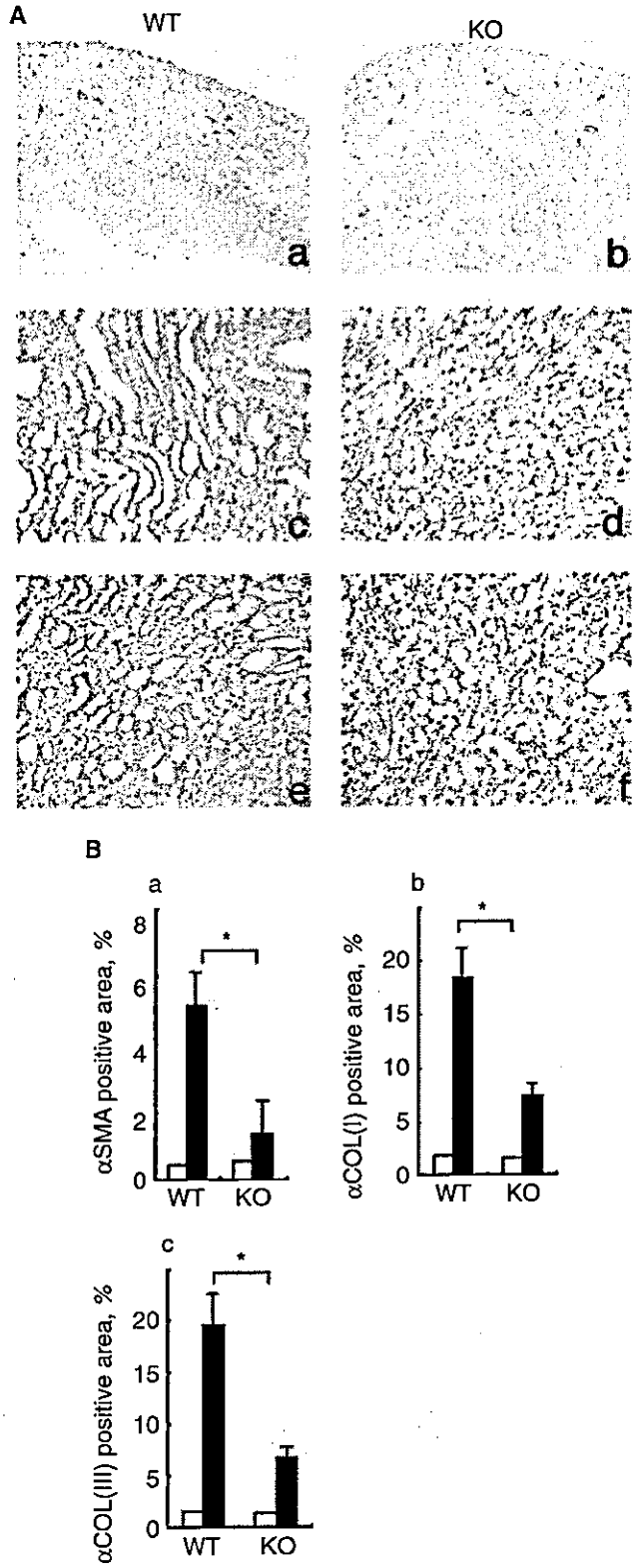

Fig. 3. Reduced number of α-smooth muscle actin (α-SMA)–positive cells or deposition of type I and type III collagens in the obstructed kidney of Smad3(−/−) mice after unilateral ureteral obstruction (UUO). (*A*) Representative pictures showing immunohistochemical staining with anti-α−SMA (a and b), anti-type I collagen (c and d), or anti-type III collagen (e and f) antibody of the kidney sections from Smad3(+/+) mice [wild-type (WT) left panels] and Smad3(−/−) mice [knockout (KO) right panels] 14 days after UUO. (*B*) Quantitative analysis of α-SMA, type I collagen, or type III collagen positive areas. The α-SMA (a), type I collagen (b), or type III collagen (c) positive area of one slide of the left obstructed (■) or nonobstructed right kidney (□) of Smad3(+/+) mice (WT) and Smad3(−/−) mice (KO) 14 days after UUO was measured with a computerized image analyzer as described in the **Methods** section. The results were expressed as percentage of positive area of one slide ($N = 6$). $^*P < 0.05$.

reduction of scar formation (whitish area in the kidney) in the obstructed kidney of Smad3(−/−) mice after UUO when compared with that of Smad3(+/+) mice. Interestingly, the size of hydronephrosis was bigger in Smad3(−/−) mice than that of Smad3(+/+) mice, suggesting that urine secretion/absorption (or renal function) was relatively maintained in Smad3(−/−) mice. Indeed, there was significant difference in the urine volume deposited in hydronephrosis between Smad3(+/+) mice and Smad3 (−/−) mice [urine volume Smad3(+/+) mice 196.7 ± 32.3 μL versus Smad3(−/−) mice 591.7 ± 149.1 μL, $P = 0.03$, $N = 6$]. Histologically, quantitative analysis of Aniline-blue or Sirius red staining after UUO revealed that the obstructed kidney of Smad3(−/−) mice had significantly reduced the staining intensity when compared with that of Smad3(+/+) mice (Fig. 2B).

It is now clear that myofibroblasts, a subpopulation of specialized fibroblasts which express the smooth muscle isoform of α-actin (α-SMA), play a central role in the mediation of tissue fibrosis with their augmented ability to produce ECM and contraction [13]. The number of interstitial myofibroblasts (α-SMA–positive cells) was increased in the obstructed kidney of Smad3(+/+) mice after UUO as previously described [23], but the intensity of the response was significantly attenuated in the obstructed kidney of Smad3(−/−) mice (Fig. 3). In addition, deposition of type I and type III collagens were significantly decreased in the obstructed kidney of Smad3(−/−) mice (Fig. 3)

Renal inflammation

Hematoxylin-eosin staining of the kidney sections suggested reduced inflammation after UUO in the obstructed kidney of Smad3(−/−) mice when compared with that of Smad3(+/+) mice (Fig. 2). The finding was supported by quantitative analysis of the number of F4/80-positive interstitial macrophages, CD4-postive T cells, and CD8-positive T cells showing reduced number of these inflammatory cells in the obstructed kidney of Smad3(−/−) mice when compared with that of Smad3(+/+) mice (Fig. 4).

Renal apoptosis

To determine renal tubular apoptosis after UUO, the TUNEL assay was performed in paraffin-embedded

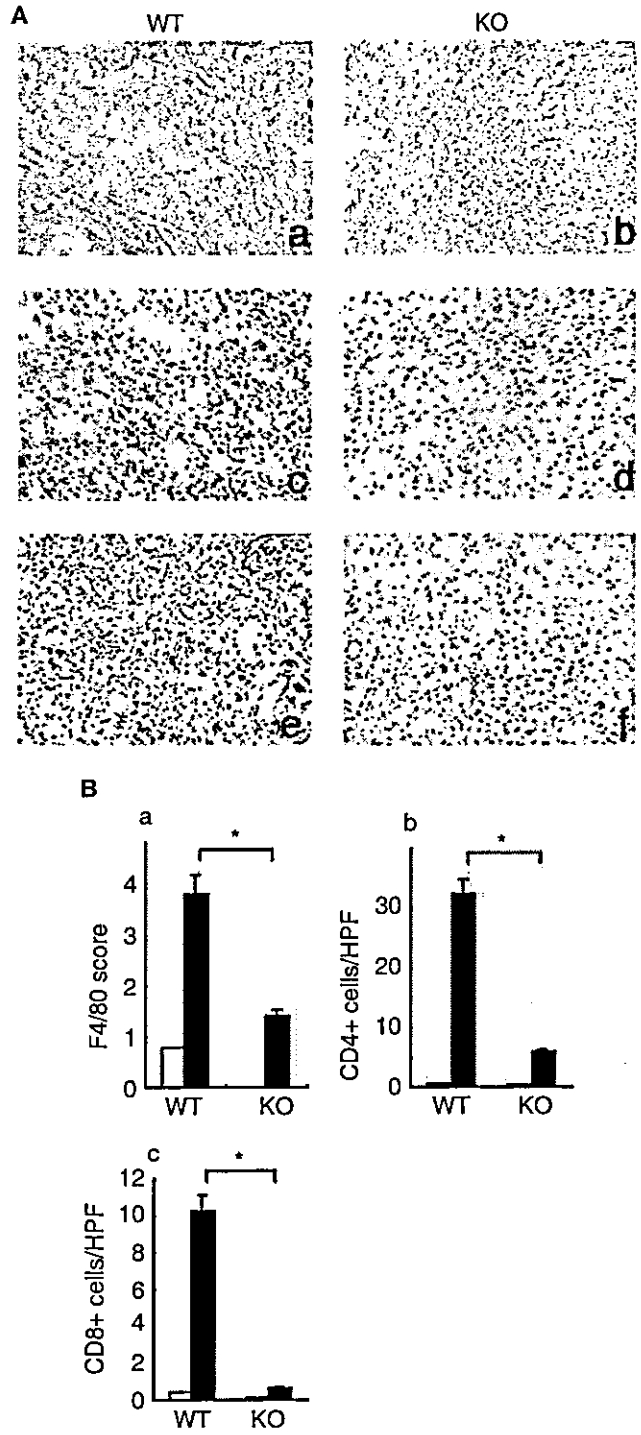

Fig. 4. Reduced renal inflammation in the obstructed kidney of Smad3(−/−) mice after unilateral ureteral obstruction (UUO). (*A*) Representative pictures showing immunohistochemical staining with anti-F4/80 (a and b), CD4 (c and d), and CD8 (e and f) antibodies of the obstructed kidney sections from Smad3(+/+) (a, b, and c) or Smad3(−/−) (d, e, and f) mice 14 days after UUO. (*B*) Quantitative analysis of immunohistochemical staining with anti-F4/80, CD4, and CD8 antibodies. (a) Scoring of the F4/80-positive cells of the left obstructed (■) or nonobstructed right kidney (□) of the mice 14 days after UUO was determined as described in the **Methods** section. (b) and (c) The number of CD4 or CD8-positive interstitial cells of the left obstructed (■) or nonobstructed right kidney (□) of the mice 14 days after UUO was counted in six random fields under high performance fields. Wild-type (WT), Smad3(+/+) mice; knockout (KO), Smad3(−/−) mice ($N = 6$). $^*P < 0.05$.

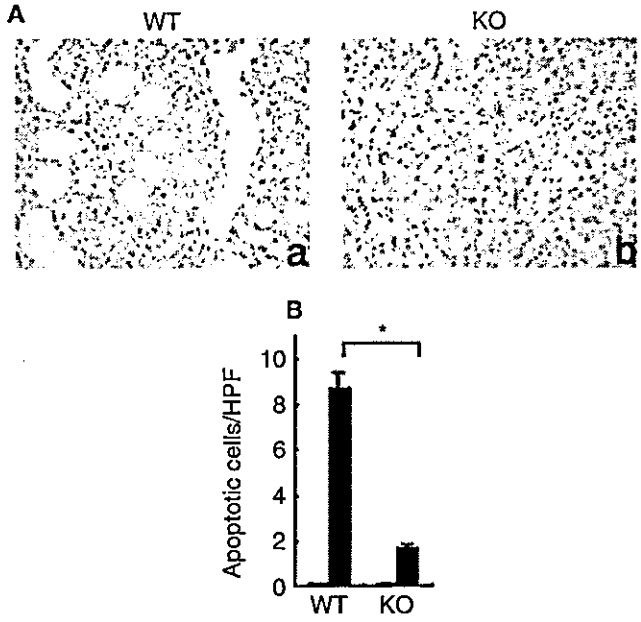

Fig. 5. Reduced tubular apoptosis in the obstructed kidney of Smad3(−/−) mice. (*A*) Representative pictures showing terminal deoxynucleotidyltransferase-mediated deoxyuridine triphosphate (dUTP) nick-end labeling (TUNEL) staining of the obstructed kidney of Smad3(+/+) mice (a) and Smad3(−/−) mice (b) 14 days after unilateral ureteral obstruction (UUO). (*B*) Quantitative analysis of tubular apoptotic cells. The number of TUNEL-positive cells was counted in six random high power fields of the left obstructed (■) or nonobstructed right kidney (□) of Smad3(+/+) mice [wild-type (WT)] and Smad3(−/−) mice [knockout (KO)] 14 days after UUO ($N = 6$). $^*P < 0.05$.

kidney sections of the mice 14 days after UUO (Fig. 5). The obstructed kidney of Smad3(+/+) mice showed significant higher tubular apoptosis when compared with nonobstructed kidney of the mice as previously described [8]. Similar to the findings in renal fibrosis and inflammation, the obstructed kidney of Smad3(−/−) mice showed significantly lower tubular apoptosis than that of Smad3(+/+) mice.

Activation of the Smad pathway after UUO

Since the data described above suggested that the Smad pathway was crucial for the development of UUO, we asked whether the Smad pathway was indeed activated in the obstructed kidney after UUO. Because of limited availability of antibodies against phosphorylated Smad3 suitable for immunohistochemical staining, we performed immunohistochemical analysis with antibody against phosphorylated Smad2, another marker for activation of TGF-β signaling. As shown in Figure 6, the

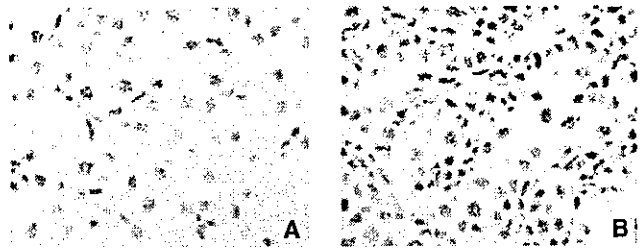

Fig. 6. Increased phosphorylated Smad2-positive cells in renal interstitial tissue after unilateral ureteral obstruction (UUO). Immunohistochemical staining with antiphosphorylated Smad2 antibody was performed in the right nonobstructed kidney (*A*) and left obstructed kidney (*B*) of wild-type mice 14 days after UUO.

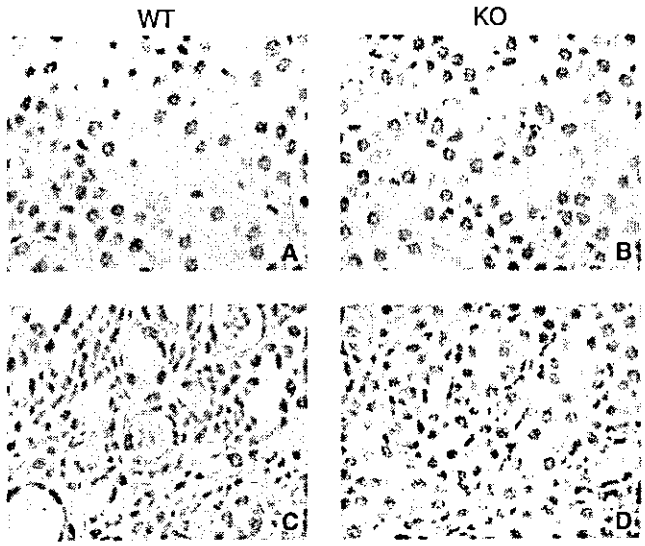

Fig. 7. Increased phosphorylated Smad2/3-positive cells in renal interstitial area after unilateral ureteral obstruction (UUO). Immunohistochemical staining with antibody cross-reacted with phosphorylated Smad2 and phosphorylated Smad3 was performed in the right nonobstructed kidney (*A* and *B*) and left obstructed kidney (*C* and *D*) of Smad3(+/+) mice [wild-type (WT)] and Smad3(−/−) mice [knockout (KO)] 14 days after UUO.

immunoreactivity of phosphorylated Smad2 was prominent in the nucleus of cells in the interstitial area of the kidney after UUO. Morphologic examination suggested that the positive staining cells observed after UUO induction were mostly infiltrated inflammatory cells and fibroblast-like cells. Thus, UUO-dependent activation of Smad2 appeared to occur largely in the cells located or infiltrated in renal interstitial area. Interestingly, renal tubular cells appeared to be constitutively positive for phosphorylated Smad2 staining independent of UUO induction. To further ascertain these results, we performed immunohistochemical analysis with antibody against phosphorylated Smad2/3 and had essentially similar results (Fig. 7). These findings indicated that activation of the Smad pathway indeed occurred in renal interstitial cells after UUO.

DISCUSSION

In this study, we demonstrated that Smad3 deficiency remarkably attenuated renal fibrosis, inflammation, and apoptosis induced by UUO (Figs. 1 to 5). In addition, we showed that endogenous Smad2/3 pathway in renal interstitial area was indeed activated after UUO (Figs. 6 and 7). Thus, we concluded that Smad3 was a key mediator for the development of UUO.

Previous in vitro studies suggested that Smad3 was critical for important aspects of TGF-β–mediated fibrotic, inflammatory, and apoptotic responses, including ECM production from fibroblasts [25], differentiation from fibroblasts to myofibroblasts [25], and chemotaxis of macrophages [27] and induction of cellular apoptosis [28], all of which were down-regulated in the obstructed kidney of Smad3(−/−) mice after UUO (Figs. 1 to 5). Our findings thus suggested that Smad3 mediated these activities in vivo as well as in vitro. It is most likely that Smad3 deficiency attenuated pathologic changes in the kidney after UUO through suppression of these cellular and molecular events.

The role of Smad3 in the differentiation of myofibroblasts (α-SMA–positive cells) is yet controversial; one paper suggested Smad3 as critical for α-SMA expression [26], other papers suggested Smad2 [29] or Smad-independent pathways [13] as important for myofibroblast differentiation. Because we showed that the number of myofibroblast in the obstructed kidney after UUO was significantly reduced in Smad3(−/−) mice (Fig. 3), it should be determined in future study whether the reduction of myofibroblast number was the direct or indirect effect of Smad3 deficiency on myofibroblast differentiation.

Renal interstitial inflammation was remarkably suppressed in the obstructed kidney of Smad3(−/−) mice as demonstrated by hematoxylin-esoin and periodic acid-Schiff staining and the number of infiltrating macrophages and T cells into the kidney (Figs. 2 and 4). Because Smad3 was critical for macrophage/monocyte chemotaxis [27, 30], the inhibition of macrophage migration into the obstructed kidney was most likely due to reduced macrophage/monocyte chemotaxis in the absence of Smad3. Although the role of Smad3 in T-cell chemotaxis remains unclear, it is possible that reduction of T-cell migration occurred through reduced production of cytokines/chemokines from macrophages involved in T-cell chemotaxis.

TUNEL assay showed clear reduction of tubular apoptosis in the obstructed kidney of Smad3(−/−) mice (Fig. 5). Renal tubular apoptosis after UUO was thought

to contribute to the progressive loss of renal function and accumulation of ECM surrounding the lost cells [3]. Our findings clearly showed that Smad3 was involved in renal tubular apoptosis in vivo. However, recently, Dai, Yang, and Liu [31] reported that TGF-β potentiated renal tubular epithelial cell death by a mechanism independent of Smad signaling. It should be therefore determined whether Smad3 was directly or indirectly involved in induction of renal tubular apoptosis in vivo.

We found that endogenous Smad2 or Smad2/3 was phosphorylated in cells located or infiltrated in renal interstitial area upon UUO induction in wild-type mice (Figs. 6 and 7). Thus, UUO-dependent activation of Smad2 appeared to occur largely in the cells in renal interstitial area. These results were consistent with upregulation of TGF-β in renal interstitial tissue after UUO as previously described [32]. Mizuno, Matsumoto, and Nakamura [32] reported that interstitial cells positive for TGF-β (e.g., macrophages, spindle-shaped fibroblast-like cells) were noted in the interstitial area of the mouse kidney after UUO. In addition, we noted that renal tubular cells appeared to be constitutively positive for phosphorylated Smad2 staining regardless of UUO induction (Fig. 6). Future studies should thus determine the biologic significance of constitutive endogenous Smad2 activation in renal epithelial cells as well as that of activation of endogenous Smad2 in renal interstitial area after UUO.

Lan et al [33] recently showed that gene transfer of Smad7, an inhibitor of TGF-β/Smad signaling, into the kidney inhibited renal fibrosis induced by UUO in rats. Most recently, Sato et al [34] reported that Smad3 deficiency protected against renal tubulointerstitial fibrosis induced by unilateral ureteral obstruction associated with blockade of epithelial-mesenchymal transition (EMT) as judged by α-SMA staining, abrogation of monocyte influx and collagen accumulation, which was essentially same findings as ours. Taken together with our findings, Smad3 is most likely to be a key mediator for renal fibrosis induced by UUO.

CONCLUSION

We clearly showed that Smad3 deficiency remarkably attenuated renal fibrosis, inflammation, and apoptosis induced by UUO. Modulation of Smad3 expression/or activity may therefore become potential therapeutic target for efficient therapy for obstructed kidney diseases or renal fibrosis.

ACKNOWLEDGMENTS

We thank Dr. C. Deng for providing us with Smad3 deficient mice, Dr. H. Ushio, Dr. C. Nishiyama, Dr. T. Takai, Dr. K. Maeda, Dr. T. Tokura, Dr. K. Yokote, and Dr. K. Kobayashi for helpful discussion and technical assistance, and M. Matsumoto and E. Kawasaki for secretarial assistance. This work was supported in part by the grant from the Ministry of Education, Culture, Sports, Science, and Technology, Japan and from the Ministry of Health, Labor, and Welfare, Japan.

Reprint requests to Atsuhito Nakao, Department of Immunology, Faculty of Medicine, University of Yamanashi, 1110, Shimokato, Tamaho, Yamanashi 409–3898, Japan.
E-mail: anakao@yamanashi.ac.jp

REFERENCES

1. Klahr S, Schreiner G, Ichikawa I: The progression of renal disease. *N Engl J Med* 318:1657–1666, 1988
2. Eddy AA: Molecular insight into renal interstitial fibrosis. *J Am Soc Nephrol* 7:2945–2508, 1996
3. Klahr S, Morrissey J: Obstructive nephropathy and renal fibrosis. *Am J Physiol Renal Physiol* 283:F861–F875, 2002
4. Walton G, Buttyan R, Garcia ME, *et al*: Renal growth factor expression during the early phase of experimental hydronephrosis. *J Urol* 148:510–514, 1992
5. Diamond JR, Kees FD, Ding G, *et al*: Macrophages, monocyte chemoattractant peptide-1, and TGF-β1 in experimental hydronephrosis. *Am J Physiol Renal Fluid Electrolyte Physiol* 266:F874–F881, 1993
6. Kaneto H, Morrissey J, Klahr S: Increased expression of TGF-β1 mRNA in the obstructed kidney of rats with unilateral ureteral ligation. *Kidney Int* 44:313–321, 1993
7. Sutaria PM, Ohebshalom M, McCaffrey TA, *et al*: Transforming growth factor-β receptor type I and II are expressed in renal tubules and are increased after chronic unilateral ureteral obstruction. *Life Sci* 62:1965–1972, 1998
8. Miyajima A, Chen J, Lawrence C, *et al*: Antibody to transforming growth factor-β ameliorates tubular apoptosis in unilateral ureteral obstruction. *Kidney Int* 58:2301–2313, 2000
9. Isaka Y, Tsujie M, Ando Y, *et al*: Transforming growth factor-β1 antisense oligonucleotides block interstitial fibrosis in unilateral ureteral obstruction. *Kidney Int* 58:1885–1892, 2000
10. Fukuda K, Yoshitomi K, Yanagida T, *et al*: Quantification of TGF-β1 mRNA along rat nephron in obstructive nephropathy. *Am J Physiol Renal Physiol* 281:F513–F521, 2001
11. Border W, Noble N: Transforming growth factor-β in tissue fibrosis. *N Engl J Med* 331:1286–1292, 1994
12. Schnaper HW, Hayashida T, Hubchak SC, Poncelet AC: TGF-β signal transduction and mesangial cell fibrosis. *Am J Physiol Renal Physiol* 284:F243–F252, 2003
13. Tomasek JJ, Gabbiani G, Hinz B, *et al*: Myofibroblasts and mechanoregulaton of connective tissue remodeling. *Nature Rev Mol Cell Biol* 3:349–363, 2002
14. Heldin CH, Miyazono K, ten Dijke P: TGF-β signaling from cell membrane to nucleus through SMAD proteins. *Nature* 390:465–471, 1997
15. Massague J: How cells read TGF-β signals. *Nat Rev Mol Cell Biol* 1:169–178, 2000
16. Attisano L, Warana JL: Smads as transcriptional co-modulators. *Curr Opin Cell Biol* 12:235–243, 2000
17. Yang X, Letterio JJ, Lechleider RJ, *et al*: Targeted disruption of SMAD3 results in impaired mucosal immunity and diminished T cell responsiveness to TGF-β. *EMBO J* 18:1280–1291, 1999
18. Datto MB, Frederick JP, Pan L, *et al*: Targeted disruption of Smad3 reveals an essential role in transforming growth factor-β-mediated signal transduction. *Mol Cell Biol* 19:2495–2504, 1999
19. Zhu Y, Richardson JA, Parada LF, *et al*: Smad3 mutant mice develop metastatic colorectal cancer. *Cell* 94:703–714, 1998
20. Nomura M, Li E: Smad2 role in mesoderm formation, left-right patterning, and craniofacial development. *Nature* 393:786–790, 1998
21. Waldrip WR, Bikoff EK, Hoodless PA, *et al*: Smad2 signaling in extraembryonic tissues determines anterior-posterior polarity of the early mouse embryo. *Cell* 92:797–808, 1998
22. Weinstein M, Yang X, Li C, *et al*: Failure of egg cylinder elongation and mesoderm induction in mouse embryos lacking the tumor suppressor Smad2. *Proc Natl Acad Sci USA* 95:9378–9383, 1998
23. Fujimoto M, Maezawa Y, Yokote K, *et al*: Mice lacking Smad3 are

protected against streptozotocin-induced diabetic glomerulopathy. *Biochem Biophys Res Commun* 305:1002–1007, 2003
24. Oda T, Jung YO, Kim HS, *et al*: PAI-1 deficiency attenuates the fibrogenic response to ureteral obstruction. *Kidney Int* 30:587–596, 2001
25. Verrecchia F, Mauviel A: Transforming growth factor-β signaling through the Smad pathway: Role in extracellular matrix gene expression and regulation. *J Invest Dermatol* 118:211–215, 2002
26. Hu B, Wu Z, Phan SH: Smad3 mediates transforming growth factor-β induced α-smooth muscle actin expression. *Am J Resp Cell Mol Biol* 29:397–404, 2003
27. Ashcroft GS, Yang X, Glick AB, *et al*: Mice lacking Smad3 show accelerated wound healing and an impaired local inflammatory response. *Nat Cell Biol* 1:260–266, 1999
28. Yang YA, Tang B, Robinson G, *et al*: Smad3 in the mammary epithelium has a nonredundant role in the induction of apoptosis, but not in the regulation of proliferation or differentiation by transforming growth factor-β. *Cell Growth Differ* 13:123–130, 2002
29. Evans RA, Tian YC, Steadman R, Phillips AO: TGF-β1-mediated fibroblast-myofibroblast terminal differentiation-the role of Smad proteins. *Exp Cell Res* 282:90–100, 2003
30. Letterio JJ, Roberts AB: Regulation of immune responses by TGF-β. *Annu Rev Immunol* 16:137–154, 1998
31. Dai C, Yang J, Liu Y: Transforming growth factor-β1 potentiates renal tubular epithelial death by a mechanism independent of Smad signaling. *J Biol Chem* 278:12537–12545, 2003
32. Mizuno S, Matsumoto K, Nakamura T: Hepatocyte growth factor suppresses interstitial fibrosis in a mouse model of obstructive nephropathy. *Kidney Int* 59:1304–1314, 2001
33. Lan HY, Mu W, Tomita N, *et al*: Inhibition of renal fibrosis by gene transfer of inducible Smad7 using ultrasound-microbubble system in rat UUO model. *J Am Soc Nephrol* 14:1535–1548, 2003
34. Sato M, Muragaki Y, Saika S, *et al*: Targeted disruption of TGF-β1/Smad3 signaling protects against renal tubulointerstitial fibrosis induced by unilateral ureteral obstruction. *J Clin Invest* 112:1486–1494, 2003

Induction of RANTES by TWEAK/Fn14 Interaction in Human Keratinocytes

Long Jin,*† Atsuhito Nakao,*‡ Masafumi Nakayama,§ Noriko Yamaguchi,§ Yuko Kojima,# Nobuhiro Nakano,* Ryoji Tsuboi,† Ko Okumura,*§ Hideo Yagita,§ and Hideoki Ogawa*¶

*Atopy (Allergy) Research Center, Juntendo University School of Medicine, Tokyo, Japan; †Department of Dermatology, Tokyo Medical University, Tokyo, Japan; ‡Department of Immunology, Faculty of Medicine, University of Yamanashi, Yamanashi, Japan; §Department of Immunology, Juntendo University School of Medicine, Tokyo, Japan; ¶Department of Dermatology, Juntendo University School of Medicine, Tokyo, Japan; #Division of Pathology, Central Laboratory of Medical Sciences, Juntendo University School of Medicine, Tokyo, Japan

TNF-like weak inducer of apoptosis (TWEAK), a member of the tumor necrosis factor (TNF) family, is a multifunctional cytokine that regulate cellular proliferation, angiogenesis, inflammation, and apoptosis. In this study, we investigated the effect of TWEAK on human keratinocytes. Primary cultured normal human keratinocytes constitutively expressed a TWEAK receptor, fibroblast growth factor-inducible 14 (Fn14), and produced regulated on activation, normal T expressed and secreted (RANTES) upon TWEAK stimulation in a concentration-dependent manner. The TWEAK-induced RANTES production was abrogated by anti-Fn14 antibody, and synergistically augmented by simultaneous stimulation with transforming growth factor-β. In addition, human keratinocytes differentiated *in vitro* with high Ca^{2+}-containing medium showed enhanced production of RANTES upon TWEAK stimulation. Furthermore, TWEAK induced rapid phosphorylation of IκB-α in human keratinocytes. Collectively, TWEAK acts on human keratinocytes as an inducer of RANTES via Fn14. Because RANTES has been implicated in inflammation, TWEAK/Fn14 interaction in human keratinocytes may be involved in the pathophysiology of inflammatory skin disorders.

Key words: keratinocytes/RANTES/TGF-β/TWEAK
J Invest Dermatol 122:1175–1179, 2004

TNF-like weak inducer of apoptosis (TWEAK) was first identified as a new member of the tumor necrosis factor (TNF) superfamily which induced cell death in some tumor cell lines (Chicheportiche *et al*, 1997; Schneider *et al*, 1999; Nakayama *et al*, 2000). The human TWEAK gene is expressed in many different cell types and encodes a ~30 kDa type II transmembrane protein that can be cleaved to generate a ~18 kDa soluble factor with biological activity. Recently, Wiley *et al* (2001) have identified fibroblast growth factor-inducible 14 (Fn14) as a TWEAK receptor with physiological affinity. Fn14 is a type I transmembrane protein composed of only one cysteine-rich domain in the extracellular region and a short cytoplasmic region containing a TNF receptor-associated factor (TRAF)-binding motif. Saitoh *et al* (2003) recently reported that TWEAK stimulates two nuclear factor-κB (NF-κB) signaling pathways: IκB-α phosphorylation and p100 processing via TRAF molecules. These findings have suggested that TWEAK has other biological functions associated with NF-κB activation than regulating cell death.

Recent evidence indeed reveals that TWEAK is a multifunctional cytokine that regulated cellular proliferation, angiogenesis, and inflammation (Wiley and Winkles, 2003). Lynch *et al* (1999) reported that TWEAK induced proliferation of endothelial cells and angiogenesis. We also reported that TWEAK upregulated cell surface expression of adhesion molecules and induced secretion of chemokines such as interleukin (IL)-8 and monocyte chemotactic protein (MCP)-1 in human umbilical vein endothelial cells (HUVEC) (Harada *et al*, 2002). Furthermore, TWEAK induced several cytokines/chemokines such as IL-8, inducible protein (IP)-10, and regulated on activation, normal T expressed and secreted (RANTES) in human dermal fibroblasts and synoviocytes (Chicheportiche *et al*, 2002). Furthermore, TWEAK induced several cytokines/chemokines such as IL=8, IP=10, and RANTES in human dermal fibroblasts and synoriocytes (Chicheportiche *et al*, 2002).

In this study, we investigated Fn14 expression on human keratinocytes and examined the effect of TWEAK on chemokine production by human keratinocytes. We found that TWEAK stimulated human keratinocytes to produce a CCL chemokine, RANTES, via Fn14. Thus, TWEAK acts on human keratinocytes as an inducer of RANTES. Because RANTES is a potent chemoattractant for leukocytes and has been associated with a wide range of inflammatory disorders (Homey and Zlotnik, 1999; Zlotnik and Yoshie, 2000; Appay and Rowland-Jones, 2001), TWEAK/Fn14 interaction in human keratinocytes may be involved in pathophysiology of certain inflammatory skin diseases.

Abbreviations: Fn14, fibroblast growth factor-inducible 14; IFN-γ, interferon-γ; IL, interleukin; NF-κB, nuclear factor-κB; RANTES, regulated on activation, normal T expressed and secreted; TGF-β, transforming growth factor-β; TNF, tumor necrosis factor; TWEAK, TNF-like weak inducer of apoptosis

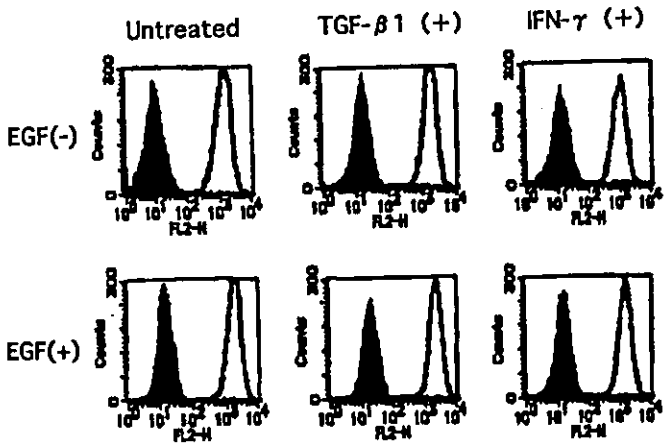

Figure 1
Cell surface expression of Fn14 on human keratinocytes. Cultured human keratinocytes were untreated or treated with 10 ng per mL of TGF-β1 or 10 ng per mL of IFN-γ for 24 h in EGF(−) or EGF(+) medium. Then, cells were stained with biotinylated anti-human Fn14 mAb (open histograms) or control Ig (filled histograms), followed by PE-labeled avidin, and then analyzed by flow cytometry. Representative of three repeated experiments with similar results were shown.

Results

Human keratinocytes constitutively express Fn14 To determine whether TWEAK may act on keratinocytes, we first examined the expression of Fn14 on cultured human keratinocytes. Flourescence activated cell sorting (FACS)-analysis using anti-Fn14 mAb showed that human keratinocytes expressed a high level of Fn14 on the cell surface, which was not affected by the presence or absence of EGF in the culture medium (Fig 1). Since Fn14 expression in endothelial cells and fibroblasts has been reported to be regulated by several growth factors and cytokines (Nakayama *et al*, 2000; Donohue *et al*, 2003; Wiley and Winkles, 2003), we next determined whether the Fn14 expression on human keratinocytes was regulated by certain cytokines. As shown in Fig 1, we found that the expression of Fn14 on keratinocytes was not affected by IFN-γ or TGF-β1.

TWEAK induces RANTES production by human keratinocytes Since cultured human keratinocytes constitutively expressed Fn14, we then investigated whether TWEAK could stimulate human keratinocytes through Fn14. Previous studies have shown that human keratinocytes could produce several chemokines that were associated with inflammatory skin diseases (Ying *et al*, 1995; Giustizieri *et al*, 2001; Horikawa *et al*, 2002). We thus examined the effect of recombinant TWEAK on IL-8, MCP-1, thymus and activation-regulated cytokine (TARC), Eotaxin, and RANTES production by human keratinocytes. As shown in Fig 2, TWEAK induced RANTES production in a concentration-dependent manner, which was almost completely inhibited by blocking the TWEAK/Fn14 interaction with anti-Fn14 mAb (Fig 2). In contrast, IL-8, MCP-1, TARC, and Eotaxin were not significantly produced in the presence or absence of TWEAK (data not shown). These findings indicated that TWEAK stimulated human keratinocytes to produce RANTES via Fn14.

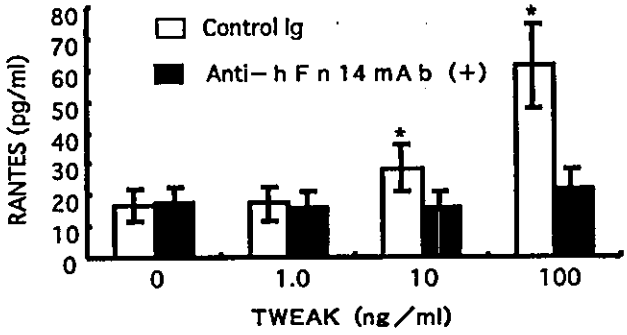

Figure 2
TWEAK induces RANTES production by human keratinocytes via Fn14. Cultured human keratinocytes were stimulated with the indicated doses of recombinant human TWEAK in the presence or absence of anti-Fn14 blocking mAb (5 μg per mL). for 48 h. Then, human RANTES concentration in the culture supernatants was measured by ELISA. Data are indicated as the mean ± SD of triplicate samples. *$p<0.05$, significantly different from the mean value of the corresponding control response. Similar results were obtained in three repeated experiments.

TGF-β synergistically augments TWEAK-induced RANTES production by human keratinocytes TGF-β has been implicated in the regulation of inflammation (Wahl, 1992) and is constitutively expressed in the human epidermis (Quan *et al*, 2002). We were thus interested in examining the effect of TGF-β on TWEAK-induced RANTES production by human keratinocytes. TGF-β1 alone modestly induced RANTES production by human keratinocytes (Fig 3). Notably, TGF-β1 showed a synergistic effect on the TWEAK-induced RANES production by human keratinocytes in a concentration-dependent manner (Fig 3). These findings indicated that TGF-β and TWEAK acted synergistically for RANTES production by human keratinocytes.

Differentiated human keratinocytes produce more RANTES upon TWEAK and TGF-β stimulation We next examined the effects of TWEAK and/or TGF-β1 on more differentiated keratinocytes. The human keratinocytes cultured in the presence of 1.2 mM Ca^{2+} for 2 d ceased proliferation, stratified and cornified as previously described (Stanley and Yuspa, 1983). As compared with the undifferentiated keratinocytes that were maintained in the culture medium containing 0.05 mM Ca^{2+}, the differentiated keratinocytes produced a comparable amount of RANTES in response to TWEAK alone but more RANTES in response to TGF-β1 alone (Fig 4). Moreover, the differentiated keratinocytes produced significantly increased amounts of RANTES in response to the combination of TWEAK and TGF-β1 (Fig 4).

Phosphorylation of IκB-α in TWEAK-stimulated human keratinocytes To explore the mechanisms by which TWEAK stimulated human keratinocytes, we investigated IκB-α phosphorylation in TWEAK-stimulated human keratinocytes. Saitoh *et al* (2003) showed that TWEAK induced phosphorylation of IκB-α, resulting in NF-κB activation in fibroblasts . As shown in Fig 5*A*, we found that TWEAK induced phosphorylation of IκB-α at 10 min after the stimulation in cultured human keratinocytes. Moreover, TWEAK and TGF-β1 showed an additive increase of

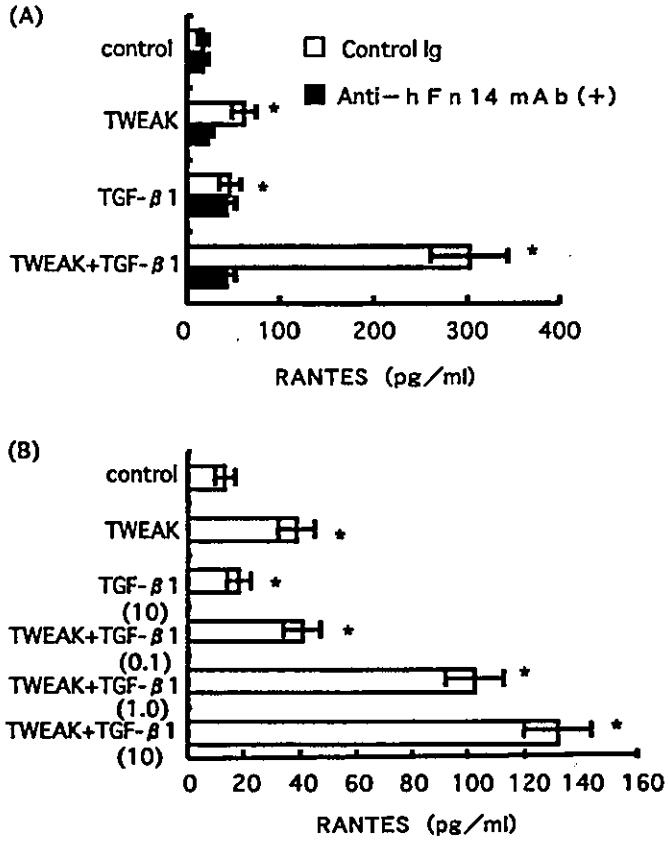

Figure 3
TGF-β1 synergizes with TWEAK for RANTES production by human keratinocytes. Cultured human keratinocytes were stimulated with 100 ng per mL of TWEAK and/or 10 ng per mL of TGF-β1 in the presence or absence of 5 μg per mL of anti-Fn14 blocking mAb (*A*) or stimulated with 100 ng per mL of TWEAK and 0.1, 1.0, or 10 ng per mL of TGF-β1 (*B*) for 48 h. Then, human RANTES concentration in the culture supernatants was measured by ELISA. Data are indicated as the mean ± SD of triplicate samples. *$p<0.05$, significantly different from the mean value of the corresponding control response. Similar results were obtained in three repeated experiments.

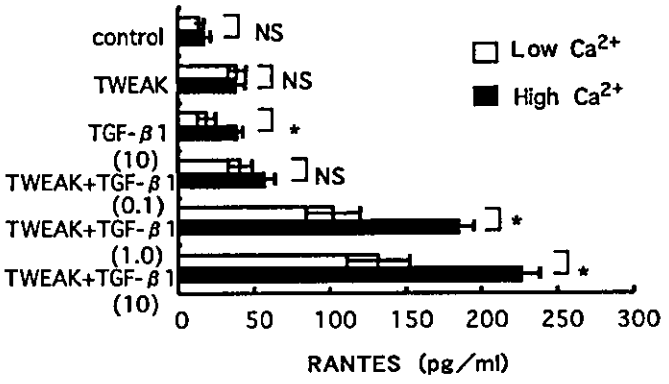

Figure 4
Differentiated keratinocytes show augmented RANTES production in response to TWEAK and TGF-β1. Human keratinocytes were cultured in the presence of 0.05 mM Ca^{2+} (white bars) or 1.2 mM Ca^{2+} (black bars) for 2 d and then stimulated with 100 ng per mL of TWEAK and 0.1, 1.0, or 10 ng per mL of TGF-β1 for 48 h. Then, human RANTES concentration in the culture supernatants was measured by ELISA. Data are indicated as the mean ± SD of triplicate samples. *$p<0.05$, significantly different from the mean value of the corresponding control response. Similar results were obtained in three repeated experiments.

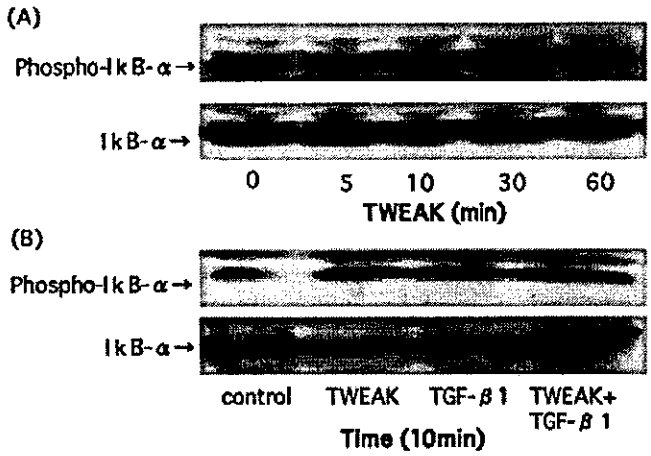

Figure 5
Phosphorylation of IκB-α in TWEAK-stimulated human keratinocytes. Cultured keratinocytes were stimulated with 100 ng per mL of TWEAK for the indicated time periods (*A*) or with 100 ng per mL of TWEAK and/or 10 ng per mL of TGF-β1 for 10 min (*B*). Then, the cell lysates were immunoblotted with anti-phosphorylated IκB-α (Ser32) antibody (upper panels) or anti-IκB antibody (lower panels). Representative of three repeated experiments with similar results.

phosphorylation of IκB-α (Fig 5*B*), which might be at least in part responsible for their synergistic action on the RANTES production.

Discussion

In this study, we demonstrated that cultured human keratinocytes expressed Fn14, which was responsible for TWEAK-induced RANTES production (Figs 1 and 2). TWEAK and TGF-β1 synergized to induce RANTES production by keratinocytes, and differentiated keratinocytes produced more RANTES in response to TWEAK and TGF-β1 (Figs 3 and 4). Because RANTES is a pro-inflammatory chemokine mediating the trafficking and homing of T cells, monocytes, eosinophils, natural killer cells, and mast cells (Homey and Zlotnik, 1999; Zlotnik and Yoshie, 2000; Appay and Rowland-Jones, 2001), these results suggest that TWEAK/Fn14 interaction in human keratinocytes may be involved in the pathogenesis of inflammatory skin disorders through RANTES production.

Cultured human keratinocytes constitutively expressed Fn14 on the cell surface (Fig 1). Because some growth factors or mitogens, including fibroblast growth factor (FGF)- and phorbol myristate acetate (PMA), regulated Fn14 expression in endothelial cells and fibroblasts (Meighan-Mantha *et al*, 1999; Donohue *et al*, 2003), we examined the influence of EGF in the keratinocyte culture and found that the Fn14 expression on human keratinocytes was not changed. We also found that IFN-γ or TGF-β1 did not affect the cell surface Fn14 expression on cultured human keratinocytes. Thus, it appeared that Fn14 expression on human keratinocytes was relatively stable as compared with endothelial cells and fibroblasts, although other growth factors or cytokines should be tested for possible regulation of Fn14 in human keratinocytes.

TWEAK induced RANTES, but not IL-8, MCP-1, TARC, and Eotaxin production in human keratinocytes (Fig 2 and

data not shown). We and others have previously shown that TWEAK induces several cytokines/chemokines; for example, IL-8 and MCP-1 from HUVEC (Harada *et al*, 2002), TNF-α from certain tumor cell lines (Nakayama *et al*, 2002), IL-8, IP-10, and RANTES from human dermal fibroblasts and synoviocytes (Chicheportiche *et al*, 2002). Thus, it seemed that the pattern of cytokines/chemokines induced by TWEAK varied depending on the cell types.

Because TGF-β has been implicated in the regulation of inflammation (Wahl, 1992) and is constitutively expressed in the human epidermis (Quan *et al*, 2002), we were interested in examining the effect of TGF-β on TWEAK-induced RANTES production by human keratinocytes. We found that TGF-β augmented TWEAK-induced RANTES production in human keratinocytes (Figs 3 and 4). Since previous studies showed that NF-κB activation resulted in upregulation of RANTES (Ebnet *et al*, 1997; Moriuchi *et al*, 1997; Ray *et al*, 1997), the findings that TWEAK and TGF-β1 showed an additive increase of phosphorylation of IκB-α (Fig 5*B*) might at least in part explain their synergistic action on the RANTES production. Alternatively, it is possible that TWEAK and TGF-β1 synergistically upregulate RANTES through their unique transcriptional factors. Indeed, synergistic effect of IFN-γ and TNF-α for RANTES production was reported in mouse fibroblasts by Ohmori *et al* (1997). They showed that IFN-γ and TNF-α synergistically upregulated RANTES through signal transducer and activator of transcription 1 (STAT1) and NF-κB, which was most likely mediated by their independent interaction with one or more components of the basal transcriptional complex.

The differentiated keratinocytes produced significantly increased amounts of RANTES in response to TGF-β1 or the combination of TWEAK and TGF-β1 as compared with undifferentiated keratinocytes (Fig 4). Thus, it appeared that differentiated keratinocytes were more susceptible to TGF-β action. Altered responses to TGF-β in undifferentiated and differentiated keratinocytes were also reported on the regulation of extracellular matrix gene expression (Vollberg *et al*, 1991). The mechanisms underlying these findings currently remain completely unclear and should be investigated in future studies.

In summary, we showed a novel biological activity of TWEAK on human keratinocytes. Because RANTES is a proinflammatory chemokine, induction of RANTES by TWEAK/Fn14 interaction in human keratinocytes may be involved in pathophysiology of certain inflammatory skin disorders.

Materials and Methods

Reagents Recombinant human TWEAK was purchased from Alexis Biochemicals (California), and recombinant human transforming growth factor-β1 (TGF-β1) and recombinant human interferon-γ (IFN-γ) were purchased from R&D Inc (Minnesota). Anti-human Fn14 monoclonal antibodies (mAb) (ITEM-1 and ITEM-2) were generated in our laboratory as previously described (Nakayama *et al*, 2003). ITEM-2 is a blocking antibody preventing the interaction between TWEAK and Fn14 (Nakayama *et al*, 2003).

Keratinocyte culture Normal human keratinocytes from infant foreskins were cultured in serum-free keratinocyte growth medium, HuMedia-KG2 (Kurabo Industries, Osaka, Japan), containing epidermal growth factor (EGF) (0.1 ng per mL), insulin (10 μg per mL), hydrocortisone (0.5 μg per mL), gentamycin (50 μg per mL), amphotericin B (50 ng per mL), and bovine brain pituitary extract (0.4%, vol/vol) at 37°C in humidified atmosphere in presence of 5% CO_2. The experiments were carried out using third- or fourth-passage keratinocytes. Induction of keratinocyte differentiation was achieved by culturing the cells for 48 h in the presence of 1.2 mM Ca^{2+} in the culture medium as previously described (Stanley and Yuspa, 1983). Keratinocyte differentiation was confirmed by morphological change.

Flow cytometric analysis for Fn14 expression Cells (1×10^6) were incubated with biotinylated anti-human Fn14 mAb (ITEM-1) for 1 h at 4°C, followed by PE-labeled avidin (BD Pharmingen, San Diego, California). After washing with PBS, the cells were analyzed on a FACSCalibur (BD Pharmingen), and the data were analyzed using the CellQuest program (BD Pharmingen).

Chemokine ELISA The amounts of IL-8, MCP-1, TARC, Eotaxin, and RANTES in the supernatant of human keratinocytes culture (1×10^6 cells/well) were determined using the ELISA kits (R&D) according to the manufacturer's instruction.

Western blot Cell lysates of cultured human keratinocytes were taken after stimulation with recombinant human TWEAK (100 ng per mL) for the indicated times and were electrophoresed on a 10% sodium dodecylsulfate–polyacrylamide gel and transferred to Immobilon-P membrane (Millipore, Billerica, Massachusetts). Immunoblotting was performed using the phosphoPlus IκB-α (Ser32) antibody kit (Cell Signaling Technology, Massachusetts) according to the manufacturer's instruction.

Data analysis Data are summarized as mean ± SD. Statistical analysis was performed using the unpaired Student's *t* test. $p<0.05$ was considered to be significant.

We thank Hiroko Ushio, Chiharu Nishiyama, Keiko Maeda, Toshiro Takai, and Tomoko Tokura for discussion and technical assistance, and Emiko Kawasaki and Michiyo Matsumoto for secretarial assistance. This work was supported in part by the grant from the Ministry of Education, Culture, Sports, Science, and Technology, Japan.

DOI: 10.1111/j.0022-202X.2004.22419.x

Manuscript received August 25, 2003; revised October 28, 2003; accepted for publication November 4, 2003

Address correspondence to: Atsuhito Nakao, Department of Immunology, Faculty of Medicine, University of Yamanashi, 1110, Shimokato, Tamaho, Yamanashi 409-3898, Japan. Email: anakao@yamanashi.ac.jp

References

Appay V, Rowland-Jones SL: RANTES: A versatile and controversial chemokine. Trends Immunol 22:83–87, 2001

Chicheportiche Y, Bourdon PR, Xu H, *et al*: TWEAK, a new secreted ligand in the tumor necrosis factor family that weakly induces apoptosis. J Biol Chem 272:32401–32410, 1997

Chicheportiche Y, Chicheportiche R, Sizing I, Thompson J, Benjamin CB, Ambrose C, Dayer JM: Proinflammatory activity of TWEAK on human dermal fibroblasts and synoviocytes: Blocking and enhancing effects of anti-TWEAK monoclonal antibodies. Arthritis Res 4:126–133, 2002

Donohue PJ, Richards CM, Brown SA, *et al*: TWEAK is an endothelial cell growth and chemotactic factor that also potentiates FGF-2 and VEGF mitogenic activity. Arterioscler Thromb Vasc Biol 23:594–600, 2003

Ebnet K, Brown KD, Siebenlist UK, Simon MM, Shaw S: Borrelia burgdorferi activates NF-κB and is a potent inducer of chemokine and adhesion molecule gene expression in endothelial cells and fibroblasts. J Immunol 158:3483–3491, 1997

Giustizieri ML, Mascia F, Frezzolini A, De Pita O, Chinni LM, Giannetti A, Girolomo S: Keratinocytes from patients with atopic dermatitis and psoriasis show a distinct chemokine production profile in response to T cell-derived cytokine. J Allergy Clin Immunol 107:871–877, 2001

Harada N, Nakayama M, Nakano H, Fukuchi Y, Yagita H, Okumura K: Pro-inflammatory effect of TWEAK/Fn14 interaction on human umbilical vein endothelial cells. Biochem Biophys Res Commu 299:488–493, 2002

Homey B, Zlotnik A: Chemokines in allergy. Curr Opin Immunol 11:626–634, 1999

Horikawa T, Nakayama T, Hikita I, *et al*: IFN-γ-inducible expression of thymus and activation-regulated chemokine/CCL17 and macrophage-derived chemokine/CCL22 in epidermal keratinocytes and their roles in atopic dermatitis. Int Immunol 14:767–773, 2002

Lynch CN, Wang YC, Lund JK, Chen YW, Leal JA, Wiley SR: TWEAK induces angiogenesis and proliferation of endothelial cells. J Biol Chem 274: 8455–8459, 1999

Meighan-Mantha RL, Hsu DK, Guo Y, *et al*: The mitogen-inducible Fn14 gene encodes a type I transmembrane protein that modulates fibroblast adhesion and migration. J Biol Chem 274:33166–33176, 1999

Moriuchi H, Moriuchi M, Fauci AS: Nuclear factor-κB potently up-regulates the promoter activity of RANTES that block HIV infection. J Immunol 158:3483–3491, 1997

Nakayama M, Ishidoh K, Kojima Y, Harada N, Kominami E, Okumura K, Yagita H: Fibroblast growth factor-inducible 14 mediates multiple pathways of TWEAK-induced cell death. J Immunol 170:341–348, 2003

Nakayama M, Kayagaki N, Yamaguchi N, Okumura K, Yagita H: Involvement of TWEAK in interferon-γ-stimulated monocyte cytotoxity. J Exp Med 192:1373–1380, 2000

Nakayama M, Ishidoh K, Kayagaki N, *et al*: Multiple pathways of TWEAK-induced cell death. J Immunol 168:734–743, 2002

Ohmori Y, Schreiber RD, Hamilton TA: Synergy between IFN-γ and TNF-α in transcriptional activation is mediated by cooperation between STAT1 and NFκB. J Biol Chem 272:14899–14907, 1997

Quan T, He T, Kang S, Voorhees JJ, Fisher GJ: Ultraviolet irradiation alters transforming growth factor-β/smad pathway in human skin *in vivo*. J Invest Dermatol 119:499–506, 2002

Ray P, Yang L, Zhang DH, Ghosh SK, Ray A: Selective up-regulation of cytokine-induced RANTES gene expression in lung epithelial cells by over-exression of IκBR. J Biol Chem 272:20191–20197, 1997

Saitoh T, Nakayama M, Nakano H, Yagita H, Yamamoto N, Yamaoka S: TWEAK induces NF-κB2 p100 processing and long-lasting NF-κB activation. J Biol Chem 278:36005–36012, 2003

Schneider P, Schwngzere R, Haas E, *et al*: TWEAK can induce cell death via endogenous TNF and TNF receptor 1. Eur J Immunol 29:1785–1792, 1999

Stanley JR, Yuspa SH: Specific epidermal protein markers are modulated during calcium-induced terminal differentiation. J Cell Biol 96:1809–1814, 1983

Vollberg TM, George MD, Jetten AM: Induction of extracellular matrix gene expression in normal human keratinocytes by TGF-β is altered by cellular differentiation. Exp Cell Res 193:93–100, 1991

Wahl SM: Transforming growth factor-β (TGF-β) in inflammation: A cause and a cure. J Clin Immunol 12:61–74, 1992

Wiley SR, Cassiano L, Lofton T, *et al*: A novel TNF receptor family member binds TWEAK and is implicated in angiogenesis. Immunity 15:837–846, 2001

Wiley SR, Winkles JA: TWEAK, a member of the TNF superfamily, is a multifunctional cytokine that binds the TweakR/Fn14 receptor. Cytokine Growth Factor Rev 14:241–249, 2003

Ying S, Taborda-Barat L, Meng Q, Humbert M, Kay AB: The kinetics of allergen-induced transcription of messenger RNA for monocyte chemotactic protein-3 and RANTES in the skin of human atopic subjects: Relationship to eosinophil, T cell, and macrophage recruitment. J Exp Med 181:2153–2159, 1995

Zlotnik A, Yoshie O: Chemokines: A new classification and their role in immunity. Immunity 12:121–127, 2000